ELSEVIER

Palaeogeography, Palaeoclimatology, Palaeoecology 167 (2001) 175–199

PALAEO

www.elsevier.nl/locate/palaeo

Linking the Wasatchian/Bridgerian boundary to the Cenozoic Global Climate Optimum: new magnetostratigraphic and isotopic results from South Pass, Wyoming

W.C. Clyde[a,*], N.D. Sheldon[b], P.L. Koch[c], G.F. Gunnell[d], W.S. Bartels[e]

[a]*Department of Earth Sciences, University of New Hampshire, 56 College Road, James Hall, Durham, NH 03824-3589, USA*
[b]*Department of Geological Sciences, University of Oregon, Eugene, OR 97403, USA*
[c]*Department of Earth Sciences, University of California, Santa Cruz, CA 95064, USA*
[d]*Museum of Paleontology, University of Michigan, Ann Arbor, MI 48109, USA*
[e]*Department of Geological Sciences, Albion College, Albion, MI 49224, USA*

Received 15 March 2000; accepted for publication 28 August 2000

Abstract

New paleomagnetic and stable isotopic results from the northeastern margin of the greater Green River Basin (South Pass, Wyoming) provide a refined geochronological context for the Wasatchian/Bridgerian Land Mammal Age boundary and suggest the existence of large amplitude Milankovich-scale carbon and oxygen isotopic oscillations in this area during the early Eocene. Analysis of 55 paleomagnetic sites through a 310 m section of Wasatch, Green River, and Bridger Formations indicates several reversals that can be correlated to the Geomagnetic Polarity Time Scale using radiometric age constraints. This correlation places the Wasatchian/Bridgerian boundary in Chron C23r at about 52 Ma, approximately two million years older than previous estimates. This new correlation suggests that the mammalian turnover which characterizes the Wasatchian/Bridgerian boundary is coincident with the onset of the Cenozoic Global Climate Optimum, the warmest interval of the entire Cenozoic. Intrabasinal magnetostratigraphic correlation supports earlier claims that community composition and biostratigraphic datums of basin-margin faunas can differ significantly from coeval basin-center faunas. Oxygen and carbon isotopic composition of paleosol carbonates show in-phase cyclic variations on the order of 6 and 3.5‰, respectively. Based on the preferred magnetostratigraphic correlation, the four best-defined cycles represent 397 thousand years, indicating potential forcing by variations in orbital eccentricity. Oxygen isotopic variations may be tracking wet/dry cycles amplified by adjacent changes in levels of paleolake Gosuite. Carbon isotopic variations may be tracking the vegetative response to these climate variations. Alternative interpretations involve cyclic changes in pedogenesis, driving correlated variations in isotopic inheritance from parent (Paleozoic) carbonate material and the possibility that C_4 plants existed in marginal habitats earlier in geological time than previously thought.

Keywords: Eocene; magnetostratigraphy; Green River Basin; biostratigraphy; mammalia; stable isotopes

1. Introduction

1.1. General background

The early Eocene was the warmest period in the last 80 million years of Earth history. As such, it has

* Corresponding author. Fax: +1-603-862-2649.
E-mail addresses: will.clyde@unh.edu (W.C. Clyde), natesheldon@darkwing.uoregon.edu (N.D. Sheldon), pkoch@emerald.uscs.edu (P.L. Koch), ggunnell@umich.edu (G.F. Gunnell), wbartels@albion.edu (W.S. Bartels).

0031-0182/01/$ - see front matter
PII: S0031-0182(00)00238-8

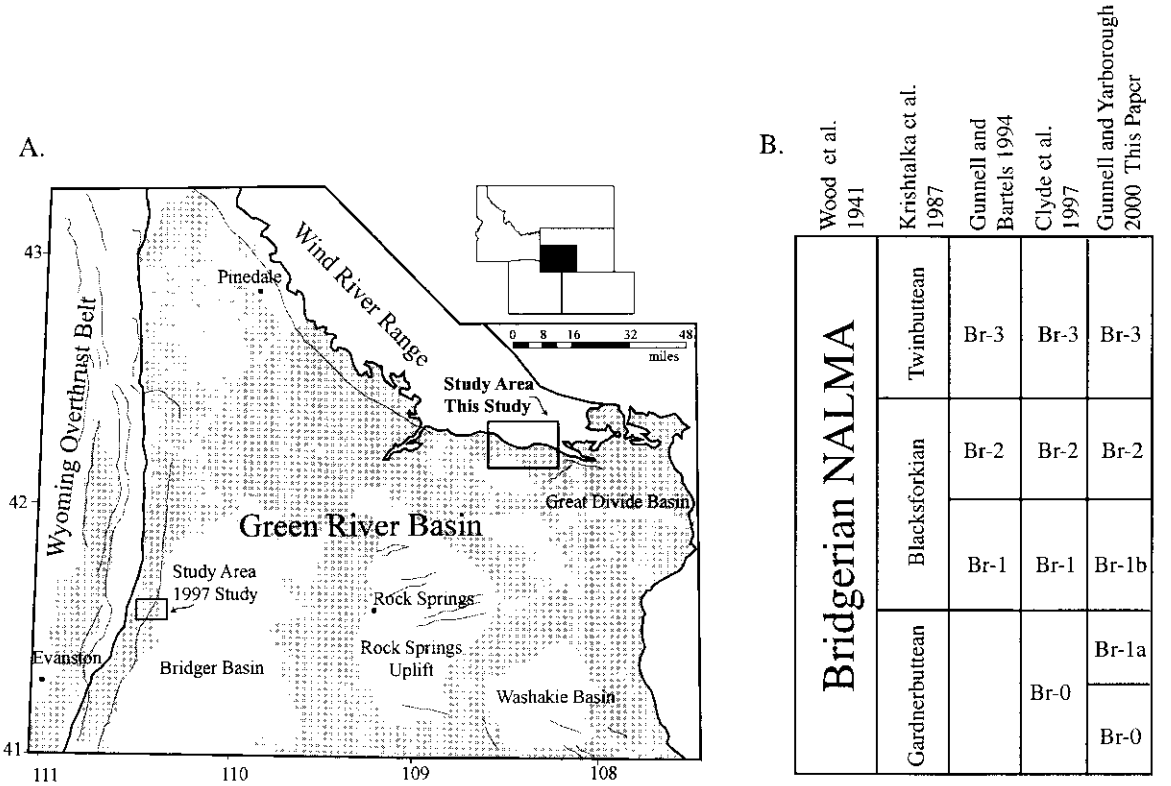

Fig. 1. (A) Map of the greater Green River Basin in southwestern Wyoming. The study area for results presented in this paper is outlined along the southern flank of the Wind River Mountains. The study area for Clyde et al. (1997) is shown in the west-central part of the basin. (B) Different biostratigraphic zonations developed for the Bridgerian Land Mammal Age.

become the focus of considerable research devoted to understanding the physiochemical causes and biological effects of globally warm climates (see Aubry et al., 1998 for review). Recent high-resolution studies of marine and continental records spanning the Paleocene/Eocene boundary have documented the existence of a short-term warming event (initial Eocene thermal maximum, IETM) that coincides precisely with a large negative excursion in the carbon isotopic composition of the mixed ocean–atmosphere–biosphere system as well as profound biotic turnover in the form of benthic foraminiferal extinction and holarctic mammalian dispersal (see Thomas and Shackleton, 1996 for review). Study of the Paleocene/Eocene boundary illustrates the importance of developing a globally integrated chronostratigraphic network that is sufficiently refined to make precise comparisons between marine and continental records of climatic and biotic change. The stratigraphic resolution required to evaluate the coincidence of these diverse patterns, however, has not been achieved for many other parts of the early Paleogene despite the existence of several other important climatic and biotic events during this interval (Thomas and Zachos, 1999). For instance, the Cenozoic Global Climate Optimum (CGCO, Berggren et al., 1998), a term referring to the long-term temperature maximum for the Cenozoic, is achieved in the later part of the early Eocene and broadly coincides with the expansion of crocodiles, arboreal mammals, broad-leaved evergreen plants, and tropical foraminifera to high latitudes (McGowran, 1990). Unfortunately, the resolution of marine and continental records through this interval is low and correlations between the realms are too imprecise to rigorously test causal hypotheses linking biotic change to climatic forcing.

The greater Green River Basin in southwestern Wyoming preserves a thick heterogeneous sequence of fossiliferous sedimentary strata spanning the early to middle Eocene (Fig. 1A). This sedimentary package provides an excellent opportunity to make close comparisons between continental and marine records of climatic and biotic change during this period of unusually warm global temperatures. A significant amount of research has been conducted on the sedimentology (Smoot, 1983; Shuster and Steidtmann, 1985; Roehler, 1990; Buchheim, 1994), stratigraphic architecture (Roehler, 1991a,b, 1992a,b), paleontology (Marsh, 1872; Cope, 1873; West, 1970; McGrew, 1971; Grande, 1984; Gunnell and Bartels, 1994; Gunnell, 1998; Zonneveld et al., 2000), and paleoclimates (Fischer and Roberts, 1991; Roehler, 1993; Norris et al., 1996; Wilf, 2000) of the greater Green River Basin. Most of these studies have sampled localities in the interior of the basin and have focused on creating a precise picture of basin evolution in order to decipher the geological and paleontological history of the northern Rocky Mountain region or to evaluate local economic potential. In this paper we evaluate the magnetostratigraphy and stable isotope stratigraphy of a basin-margin section along the Wind River uplift and focus on creating a detailed geochronology to make precise correlations between marine and continental records of climatic and biotic change. The margins of Laramide basins have received relatively little attention among stratigraphers and paleontologists, yet several studies have shown these settings to preserve unusual depositional environments and unique paleontological assemblages that can differ significantly from their basin-center counterparts (Gunnell and Bartels, 2001).

1.2. The Wasatchian/Bridgerian boundary

The Wasatchian/Bridgerian boundary represents one of the 18 major turnovers in the North American Cenozoic mammalian record. It is marked by the first appearance of nine taxa, including several perissodactyls (e.g. *Hyrachyus*, *Palaeosyops*) and primates (e.g. *Omomys*, *Smilodectes*), and corresponds to a period of relatively high North American mammalian diversity (Krishtalka et al., 1987; Stucky, 1990; Alroy, 1999). Although the early–middle Eocene is often referred to as a period of increased endemism and intracontinental diversification, the abrupt first appearance of several taxa at the Wasatchian/Bridgerian boundary had important effects on subsequent North American mammalian community structure (Krishtalka et al., 1987; Woodburne and Swisher, 1995). For instance, the endemic anaptomorphine-dominated tarsiiform primate faunas of the Wasatchian were largely replaced by an influx of omomyine taxa in the earliest Bridgerian (Gunnell, 1997). In many ways the late Wasatchian to early Bridgerian represents an important point in North American mammalian community evolution. It signifies the culmination of closed habitat 'greenhouse' faunas characteristic of much of the early Paleogene in North America. By the end of the Bridgerian (~46 Ma), North American mammalian faunas began to resemble the more open habitat 'ice-house' faunas that characterize the rest of the Cenozoic (Stucky, 1990).

Despite the importance of these events to the faunal evolution of North America, the geochronology of the Wasatchian/Bridgerian boundary remains in doubt, making it difficult to compare these patterns to those observed elsewhere in the world. A recent magnetostratigraphic study from the western part of the basin proposed two possible correlations to the Geomagnetic Polarity Time Scale (GPTS) that differed by two million years (Clyde et al., 1997). Correlation 1 placed the boundary in Chron C23r at about 52 Ma on the most recent GPTS. Correlation 2 placed the boundary in Chron C22r at about 50 Ma on the most recent GPTS. More magnetostratigraphic and/or radiometric data were needed to confidently exclude one of these two correlations. Here we report new magnetostratigraphic results from the South Pass region of the greater Green River Basin that in conjunction with a newly reported radiometric age from elsewhere in the basin (Murphey et al., 1999), help to further constrain the geochronology of the Wasatchian/Bridgerian boundary.

These alternate correlations have significant implications for our understanding of how climate change might condition faunal turnover at the boundary. In the marine record, the CGCO begins during C23r and persists through C23n (Zachos et al., 1994, personal communication), before temperatures begin their long slide toward 'ice-house' conditions. Consequently, Correlation 1 places the Wasatchian/Bridgerian

boundary coincident with the onset of the CGCO, whereas under Correlation 2, the faunal change is associated with the onset of global cooling after the CGCO.

In addition to using magnetostratigraphy to provide a tighter linkage between North American mammalian evolution and the global record of climate change, we also explore local climate change through isotopic study of paleosol carbonates. Stable isotope geochemistry of minerals precipitated organically and inorganically in continental settings have become an important resource for reconstructing aspects of ancient terrestrial ecosystems. The carbon and oxygen isotope compositions of paleosol carbonates have been especially useful for reconstructing changes in climate (Cerling, 1984; Koch et al., 1995), recording shifts in vegetational cover (Quade and Cerling, 1995), and tracking changes in the global carbon budget (Koch et al., 1992). We analyzed pedogenic carbonates from the Wasatch Formation exposed at South Pass in order to evaluate environmental change in this upland habitat during the globally warm climates of the early Eocene.

1.3. Geological and stratigraphic setting

The stratigraphic sections studied here are located in the South Pass region of Wyoming (42°13′N, 108°32′W, elev. 2200 m) on the northeast margin of the greater Green River Basin (Fig. 1A). The greater Green River Basin is a large (>50,000 km^2) intermontane basin that encompasses several smaller depositional centers (e.g. Bridger Basin, Washakie Basin, Great Divide Basin, Sand Wash Basin). It is bounded by various Laramide and Sevier style structural elements including the Wind River Mountains to the northeast, the Uinta Mountains to the south, and the Wyoming Overthrust Belt to the west. Stratigraphic architecture within the greater Green River Basin is largely controlled by flexural response to these extrabasinal loads (Hagen et al., 1985). Although synorogenic sedimentation began in this area during the Mesozoic development of the Overthrust Belt, rapid subsidence and erosional unroofing associated with bounding Laramide structures reached their maximum in the early Tertiary (Roehler, 1992c). Some of the thickest and best exposed strata in the greater Green River Basin are early to middle Eocene in age. The three generally flat-lying formations that make up the bulk of this interval are, from bottom to top, the Wasatch Formation, the Green River Formation, and the Bridger Formation.

The Wasatch Formation in the study area is part of the Cathedral Bluffs Tongue and is characterized by red/gray variegated mudstone and sandstone packages. These facies are interpreted to be fluvial overbank deposits that have undergone significant amounts of pedogenesis. The Green River Formation in the study area is part of the Laney Member and is characterized by fine-grained greenish gray shales interbedded with thin sandstones, algal laminites, and oolitic limestones. These facies are interpreted to have been deposited within a shallow lacustrine setting. Wasatch and Green River lithologies intertongue extensively throughout the Green River Basin, tracking changes in the size and shape of paleolake Gosuite (Roehler, 1992c, 1993). The Bridger Formation overlies the Wasatch and Green River Formations throughout much of the basin. It is characterized by fluvial sandstones and mudstones that include appreciable amounts of volcaniclastic detritus as well as laterally extensive lacustrine limestones and marls. Volcanic tuffs are also present in the Bridger Formation, providing excellent radiometrically constrained marker horizons (Evanoff et al., 1998). The composite section studied here encompasses approximately 120 m of Wasatch Formation, 75 m of Green River Formation, and 115 m of Bridger Formation.

Krishtalka et al. (1987) identified three subages within the Bridgerian land mammal age — the Gardnerbuttean, the Blacksforkian, and the Twinbuttean. Since that study, there have been several attempts to develop a more refined biostratigraphic zonation for the Bridgerian with the most recent system splitting the Bridgerian into 5 different biostratigraphic zones (Gunnell and Yarborough, 2000; Fig. 1B). These informal faunal zones should not be confused with the five lithostratigraphic members of the Bridger Formation (Bridger A–E) that were originally identified by Matthew (1909) and are still in wide use today.

There are a total of 75 fossil localities (1141 mammal specimens) that can be tied to the South Pass section studied here. These localities are all characterized by Bridgerian faunas and include the key Bridgerian index taxa *Paleosyops, Hyrachyus,* and

Table 1
UTM coordinates for the bottom and top of each section measured at South Pass. All coordinates are differentially corrected (via GPS) except for the top of section 98PM-7, which was estimated from a map. Coordinates are referenced to the 1927 North American Datum. Sections were correlated lithostratigraphically although there may be up to 10 m gap between sections 98PM-4 and 98PM-6

Local section	Composite section meter levels	Bottom		Top	
		Easting	Northing	Easting	Northing
98PM-1	0.00–17.25	702685.327	4676687.868	702688.429	4676762.941
98PM-2	17.25–30.00	703811.613	4677942.623	703841.658	4677959.768
98PM-3	30.00–48.95	703598.990	4678250.634	703574.323	4678279.012
98PM-4	48.95–96.10	703504.223	4678687.786	703502.172	4678825.948
98PM-5	N/A	689622.722	4660241.950	689592.495	4660073.733
98PM-6	96.10–186.50	695070.100	4678052.851	695209.558	4678898.747
98PM-7	186.50–304.00	690756.162	4681911.913	690900.000	4682000.000

Trogosus. Localities in the lowest 150 m of section exhibit typical Gardnerbuttean faunas (Zone Br1a of Gunnell and Yarborough, 2000) whereas localities above that level exhibit typical Blacksforkian faunas (Zone Br1b of Gunnell and Yarborough, 2000) although the exact boundary between these zones is poorly constrained. Complete faunal lists of the vertebrate faunas from South Pass can be found elsewhere (Gunnell and Bartels, 2001). Wasatchian faunas are found at five localities (130 specimens) in an area known as 'the Pinnacles' which lies some 20 km south/southwest of the study site and approximately 50 m stratigraphically below the base of the section described here. Classic Wasatchian taxa like *Lamdotherium* and *Cantius* are known from localities in 'the Pinnacles', indicating that the Wasatchian/Bridgerian boundary lies within this approximately 50 m covered interval.

2. Methods

2.1. Paleomagnetic analysis

Six separate stratigraphic sections (98PM1–4, 98PM6–7) were measured in the study area and correlated lithostratigraphically to form a composite section (Table 1). A sixth section (98PM5) near 'the Pinnacles' was measured below this composite section in Wasatchian aged (Lostcabinian subage) deposits but the paleomagnetic behavior and carbonate preservation of these facies (10 sites) was very poor, so that section is not discussed further. At least three oriented paleomagnetic samples were collected from 55 sites through the 310 m composite section. Average spacing between sites was 5.6 m but varied between 0.4 and 26.5 m depending on the quality of exposure and distribution of appropriate facies. Samples were taken from one of three facies: (1) red B horizons of Wasatch Formation paleosols (37 sites); (2) algal or oolitic limestones from the Green River Formation and Bridger Formation (8 sites); and (3) grayish green calcareous shales (little to no pedogenic alteration) from the Green River Formation and Bridger Formation (10 sites). Weathered material was removed from the surface before extracting samples. Samples were either drilled as oriented cores using a water cooled rock coring devise or removed as oriented hand samples and cut into approximately 8 cm^3 cubes.

Bulk susceptibility of samples was measured on a kappa bridge before demagnetization. Progressive step-wise thermal demagnetization was carried out using a Schonstedt TSD-1 thermal demagnetizer. Remanence measurements were made on a three-axis cryogenic magnetometer (2G) in the magnetically shielded paleomagnetic laboratory at the University of Michigan. Previous studies of these facies showed that thermal demagnetization proved to be more effective in isolating remanence components than AF demagnetization methods so all samples were thermally demagnetized (5–10 steps) up to a maximum temperature of 680°C. Overprint and remanence components were determined by visual inspection of vector end-point diagrams. For samples that exhibited linear decay to the origin,

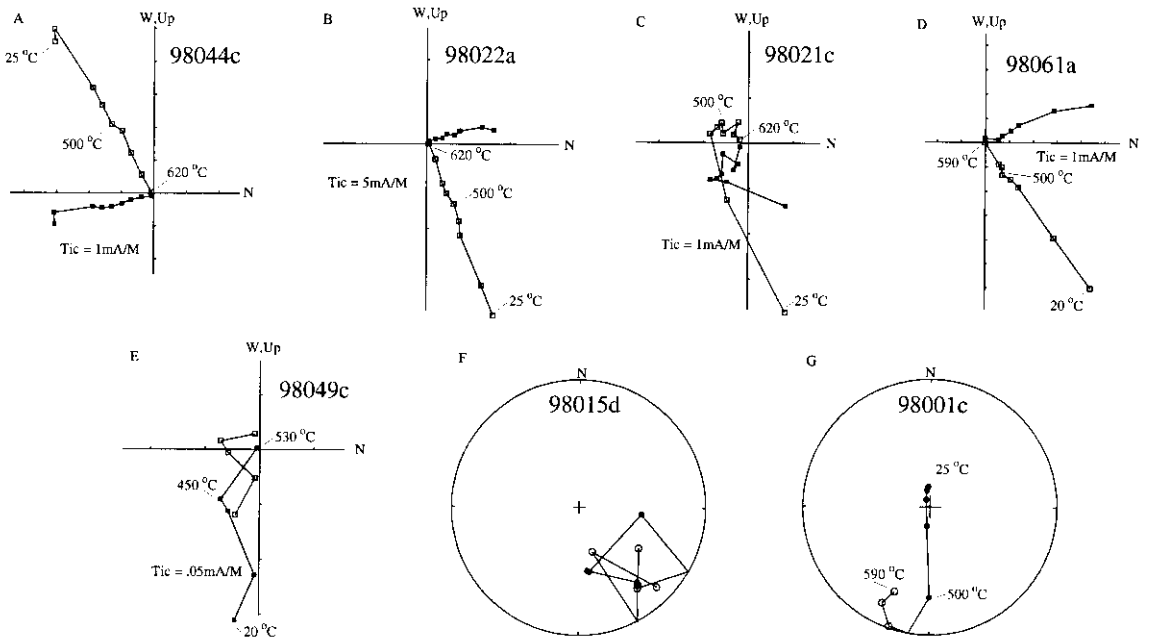

Fig. 2. (A–E) Representative vector endpoint diagrams (Zijderveld, 1967) of paleomagnetic samples analyzed from the Wasatch, Bridger, and Green River Formations. Open (closed) symbols show vector endpoints in the vertical (horizontal) plane. (A) and (B) Wasatch Formation paleosol samples showing reverse and normal characteristic magnetizations. (C) Wasatch Formation sample that exhibits an overprint component of magnetization as well as a reversed characteristic component of magnetization. (D) Siltstone sample from the Bridger Formation showing unblocking by 590°C. (E) Green River Formation sample that exhibits relatively unstable demagnetization behavior. (G) and (F) Equal area projections where open (closed) symbols lie on the upper (lower) hemisphere of the projection. (G) Wasatch formation sample that exhibits clustering of magnetic endpoints where a Fisher mean was used to calculate a ChRM direction. (F) Wasatch Formation sample representing an example of a great circle trajectory used to infer a reversed ChRM.

characteristic directions were computed using least-squares analysis (Kirschvink, 1980). Characteristic directions in nine samples that showed strong clustering of vector end-points but no linear decay to the origin were calculated using a mean. Mean directions and their surrounding statistical distributions were calculated following the method described by Fisher (1953). Sites with at least three samples exhibiting stable demagnetization that passed the Watson (1956) test for randomness at the $\alpha = 0.05$ significance level were considered as alpha sites, although all samples that exhibited stable demagnetization were used to establish the stratigraphic bounds of polarity zones.

2.2. Stable isotope analysis

Paleosol carbonates were collected from 36 sampling levels within 110 m of Wasatch Formation (Cathedral Bluffs member). Nodules were collected from at least 30 cm below the original A horizon of the paleosol. Flat surfaces were ground on nodules, then nodules were rinsed and dried. When available, two nodules were analyzed from each sampling level, and two isotopic samples were collected per nodule.

Approximately 100 μg of calcite was collected for isotopic analysis. Sample powders were collected from flat surfaces by drilling under a binocular microscope. This process helps avoid diagenetic cements, which can have isotopic values quite distinct from pedogenic carbonates (Koch et al., 1995). Sample powders were roasted at 450°C for 1 h, then analyzed on a Micromass Prism gas source mass spectrometer using an Isocarb automated carbonate analysis system. Briefly, samples are reacted in vigorously stirred 100% H_3PO_4 at 90°C for 5 min, with continual cryogenic trapping of the CO_2 and H_2O generated

by carbonate dissolution, then the CO_2 is released into the source of the mass spectrometer for analysis. Isotopic data are reported using the standard δ notation relative to V-PDB. Standardization was achieved by analysis of NBS 19 and Carrera Marble (CM), an internal laboratory standard. Standard errors for 50 analyses of CM determined concurrently with paleosol carbonates were 0.08‰ for $\delta^{18}O$ and 0.13‰ for $\delta^{13}C$.

3. Paleomagnetic results

Wasatch and Bridger Formation samples were characterized by relatively strong remanence intensities (mean $J_o = 4.6$ mA/m, excluding one outlier site that had a mean of 483 mA/m) and tended to exhibit the most stable demagnetization behavior (Fig. 2A–D). Green River Formation samples exhibited very weak natural remanent magnetizations (mean $J_o = 0.27$ mA/m) with relatively poor demagnetization behavior (Fig. 2E). This corresponds to previous paleomagnetic results from these formations (Sheriff and Shive, 1982; Clyde et al., 1997).

Most samples from the South Pass section that exhibited stable demagnetization were characterized by one or two remanence components. Those that exhibited two components usually had a present-day overprint component that was unblocked by 200°C. The characteristic component for most samples was isolated between 200 and 650°C. A few Wasatch Formation samples located stratigraphically just below reversal events exhibited antipodal remanence components that correspond to the expected Eocene direction for southeastern Wyoming (349/61, Diehl et al., 1983). This implies that remanent acquisition in these paleosols occurred over time scales greater than the duration of the reversal event. Unblocking temperature for most Wasatch Formation samples was between 620 and 680°C suggesting fine-grained hematite as the magnetic carrier. Many Bridger Formation samples had slightly lower unblocking temperatures and were characterized by strong magnetic susceptibilities suggesting magnetite was the remanence carrier. Demagnetization behavior and unblocking temperatures for Green River Formation samples suggest a highly dispersed magnetite carrier.

Of the 167 samples analyzed from the South Pass composite section, 91 samples exhibited stable demagnatization behavior and were used to establish a polarity record. The average maximum angle of deviation (MAD) for all samples for which lines were calculated was 8.6. Fig. 3 shows stereonet projections of the NRM directions before demagnetization, the characteristic components of magnetization for the samples that exhibited stable demagnetization behavior, and the mean directions for all alpha sites. Only two samples included in the alpha sites had MADs of greater than 15 ($MAD_{98031A} = 23.8$, $MAD_{98043A} = 16.2$). Table 2 shows the paleomagnetic results and corresponding statistics for the 19 alpha sites that represent the most reliable sites in the section. Both the sample directions and site directions pass the reversal test at the 95% confidence limit (McFadden and Lowes, 1981).

Fig. 4 shows the distribution of paleomagnetic pole latitudes for samples and alpha sites from the composite section studied here. Six different polarity zones are identified; polarity zone A− spans 0–17 m, polarity zone B + spans 17–56 m, polarity zone C− spans 56–80 m, polarity zone D + spans 80–95 m, polarity zone E− spans 95–235 m, and polarity zone F + spans 235–270 m. The polarity of the uppermost 35 m of the section is ambiguous due to poor sample demagnetization behavior. All polarity zones are characterized by at least one alpha site except zone D + , which is characterized by three stable samples from two closely spaced sites that exhibit congruent characteristic magnetizations. The middle of zone E− is poorly constrained due to the poor paleomagnetic behavior of Green River Formation samples yet those samples that do exhibit stable demagnetization indicate a reversed polarity for this interval. Paleomagnetic reversals do not coincide with lithological transitions or significant changes in magnetic susceptibility indicating that the polarity record is independent of rock type and magnetic mineralogy.

4. Correlation to the GPTS

For many years the Wasatchian/Bridgerian boundary was poorly constrained to lie within a broad five million year interval between 53 and

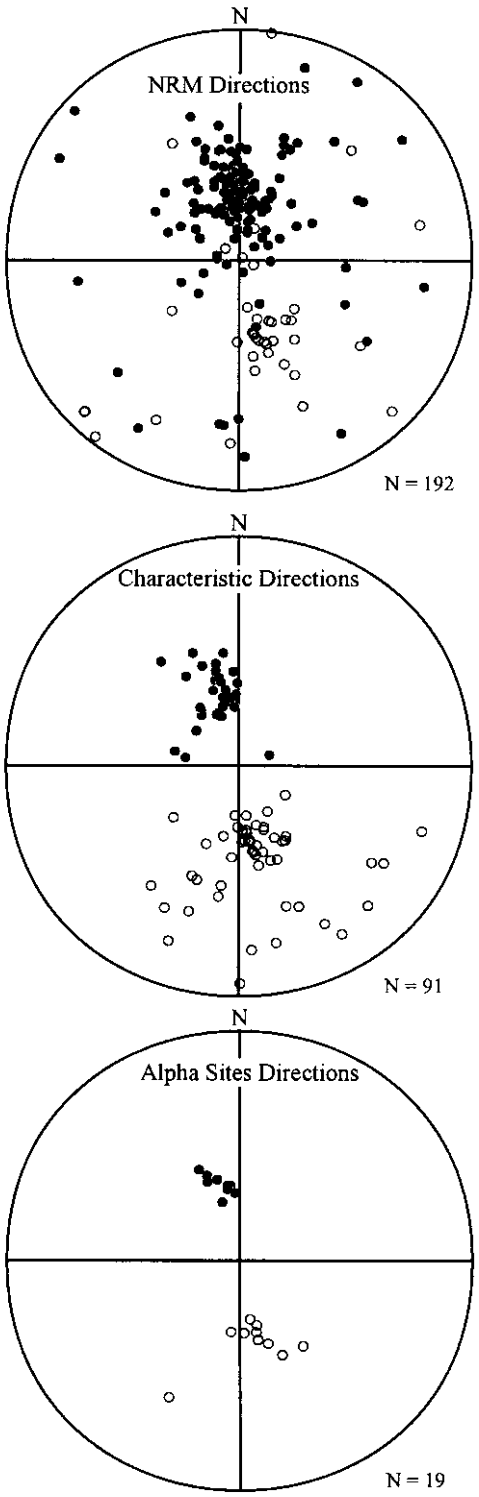

48 Ma (Butler et al., 1981; Flynn, 1986; Clyde et al., 1994; Tauxe et al., 1994; McCarroll et al., 1996; Walsh, 1996). Clyde et al. (1997; see also Zonneveld et al., 2000) studied the magnetostratigraphy of a section spanning the boundary in the southwestern part of the Green River Basin and constrained the boundary to lie within either Chron C23r (approx. 52 Ma) or C22r (approx. 50 Ma). The correlation placing it within Chron C23r (Correlation 1) provided a better match to the details of the marine polarity reversal record but required significant shifts in sediment accumulation rates throughout the section. The alternative correlation with Chron C22r (Correlation 2), which was tentatively preferred at the time, was burdened by an extra short-term reversal that was not evident in the marine record but was consistent with more uniform sediment accumulation rates through the section. The magnetic polarity record from South Pass in conjunction with a new high precision $^{40}Ar/^{39}Ar$ age from elsewhere in the basin allow us to rule out the second of these two correlations.

The South Pass section studied here stratigraphically overlaps with the upper part of the section from the 1997 Bridger Basin study (Clyde et al., 1997; Zonneveld et al., 2000). Within this overlapping interval, the ordering of lithostratigraphic, biostratigraphic, and magnetostratigraphic events is remarkably similar between these two sections (Fig. 5). Both sections preserve the Wasatchian/Bridgerian boundary within a reversed interval, both sections show a short reversed interval in the normal zone above the Wasatchian/Bridgerian boundary, and both sections preserve the contact between the Cathedral Bluffs Tongue of the Wasatch Formation and the Laney member of the Green River Formation within a relatively long reversed polarity zone. These similarities suggest that the polarity record from South Pass is robust and, most importantly, that the short reversed zone within the normal zone after the Wasatchian/Bridgerian

Fig. 3. Equal area projections of NRM directions, characteristic directions after demagnetization, and mean directions for alpha sites. Open (closed) symbols lie on the upper (lower) hemisphere of the projection. Samples and sites pass the reversal test at $\alpha = 0.05$ (McFadden and Lowes, 1981). The mean direction for all alpha sites when reversed sites are inverted is 348/61 ($\alpha_{95} = 4.6$), remarkably close to the expected early eocene direction of 349/61 (Diehl et al., 1983).

Table 2
Paleomagnetic data for alpha sites from South Pass. Meter level is from the composite section. Dec and Inc are the declination and inclination of the characteristic remanent magnetization. α_{95} represents the 95% zone of confidence. VGP lat is the latitude of the paleomagnetic pole. Zone is the local polarity zone. Polarity zone D+ is not represented by an alpha site but is represented by three stable samples from two closely spaced sites that exhibit congruent characteristic magnetizations. *R* is the length of resultant magnetic vector with two stars (**) representing a significantly nonrandom distribution at $\alpha = 0.01$ and one star (*) representing significance at $\alpha = 0.05$ (Watson 1956). Kappa is the precision parameter

Alpha site	Level (m)	Dec	Inc	α_{95}	VGP lat	Zone	*R*	Kappa
SP-99011	14.0	207.3	−33.8	11.4	−50.5	A−	2.98**	118.7
SP-99013	16.8	143.7	−52.1	36.2	−69.8	A−	2.84*	12.6
SP-99014	17.3	344.5	60.1	14.0	86.1	B+	2.97**	78.5
SP-99017	22.0	338.0	59.8	25.6	82.0	B+	2.92**	24.3
SP-99018	23.8	352.9	63.0	9.6	82.5	B+	2.99**	165.9
SP-99019	34.1	355.7	65.9	3.0	78.3	B+	3.00**	1708.3
SP-99022	51.6	343.6	68.4	4.1	76.1	B+	3.00**	886.6
SP-99023	54.0	350.9	63.0	5.6	83.1	B+	3.00**	486.1
SP-99024	55.5	350.2	64.3	3.2	81.7	B+	3.00**	465.7
SP-99031	72.2	155.8	−53.1	45.8	−79.4	C−	2.76*	8.3
SP-99043	97.4	170.0	−69.0	10.3	−75.4	E−	2.99**	145.5
SP-99044	106.8	167.2	−61.2	7.5	−85.7	E−	2.99**	271.6
SP-99045	109.5	165.3	−66.5	9.5	−78.9	E−	2.99**	168.1
SP-99046	113.3	161.2	−58.9	10.9	−84.7	E−	2.98**	129.9
SP-99056	222.4	167.1	−64.0	8.8	−82.3	E−	2.99**	198.0
SP-99058	224.5	186.9	−64.6	12.1	−73.5	E−	2.98**	105.5
SP-99059	227.3	176.7	−64.3	3.7	−79.5	E−	3.00**	1116.9
SP-99060	244.7	339.1	57.5	10.2	83.2	F+	2.99**	147.0
SP-99061	268.7	336.1	54.4	16.2	80.2	F+	2.97**	59.2

boundary (zone C− in Fig. 4) is real and should correlate to a reversal in the marine record. Of the two potential correlations outlined above, only Correlation 1 shows a perfect match between the local and marine reversal record.

A recent radiometric age from Bridger 'B' strata provides further evidence to rule out Correlation 2 from the 1997 study. The age of 47.96 ± 0.13 Ma for the Church Butte Tuff (Murphey et al., 1999), approximately 150 m above the top of the South Pass section, places the Middle Bridger 'B' near the Chron C21n/C21r boundary which is dated at 47.91 Ma (Cande and Kent, 1995). Under Correlation 2, the Chron C21n/C21r boundary would be located 65 m *below* the top of the South Pass section which is some 215 m below its predicted placement based on the new radiometric age. Alternatively, using Correlation 1 and the average sediment accumulation rate for the entire section implied by that correlation (107 m/My), an ash with an age of 47.96 Ma should lie 123 m above the top of the section — quite close to its approximate observed location of 150 m above, and well within stratigraphic error. The correlation putting the Wasatchian/Bridgerian boundary within Chron C23r is now strongly favored due to its robust match to the detailed reversal record of the GPTS and the constraints imposed by new radiometric age information. The new calibration for this part of the record makes the Bridgerian land mammal age, and particularly the Gardnerbuttean subage, significantly longer than previously assumed (with a corresponding decrease in the Lostcabinian subage of the Wasatchian) and places the Wasatchian/Bridgerian boundary in the middle part of the early Eocene (= Ypresian) rather than near the early Eocene/middle Eocene (= Ypresian/Lutetian) boundary (Fig. 6).

5. Stable isotopes

5.1. Background

Stable isotope analyses of soil and paleosol carbonates have been used extensively to track changes in

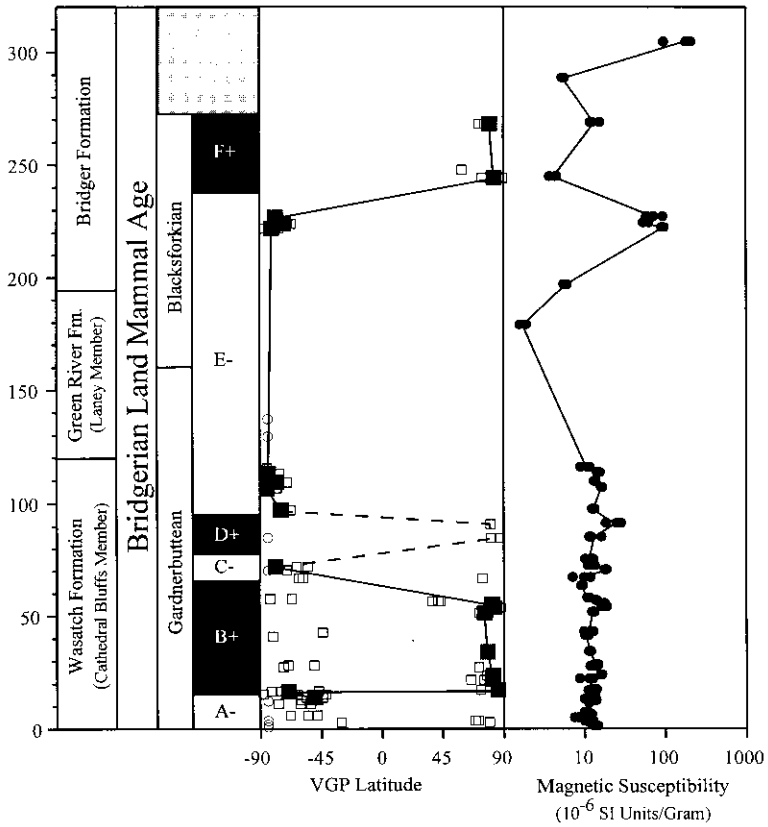

Fig. 4. VGP latitude and magnetic susceptibility plotted against lithostratigraphic and biostratigraphic units from the study section at South Pass. Solid squares represent alpha sites, open squares represent individual samples that exhibited stable demagnetization, and open circles represent samples that followed a great circle path toward a reverse direction during demagnetization. Six polarity zones are identified in the section (zones A − to F +). Polarity transitions do not correlate with changes in susceptibility or lithology suggesting that they are independent of changes in magnetic mineralogy.

continental climates, biomass, and atmospheric chemistry (Cerling, 1984; Cerling et al., 1989; Quade et al., 1989; Koch et al., 1992, 1995; Mora et al., 1996; Amundson et al., 1996). The carbonates that form relatively deep (>30 cm) in soils contain carbon that is chiefly supplied from the soil CO_2 generated by plant decomposition and root respiration (Cerling, 1984). Because soil carbonates contain carbon that is ultimately derived from the plants overlying the soils, their isotope composition tracks the composition of this vegetation (Cerling and Quade, 1993). Prior work has investigated the potential complications introduced by two sources of carbon not derived from the overlying biomass, atmospheric CO_2 and detrital carbonate. In moderately to highly productive soils, ^{13}C-enriched atmospheric CO_2 only influences carbonates formed at the very top of the soil, though, under conditions of higher atmospheric pCO_2, this effect may penetrate deeper into soils (Quade et al., 1989; Cerling, 1992). For well developed soils in clastic settings, detritial carbonate is leached away during pedogenesis and does not affect the isotope composition of carbonates retrieved from soils (Quade et al., 1989). Thus when sampled with care, paleosol carbonates may supply information about changes in the isotopic composition of overlying vegetation.

The $\delta^{13}C$ of surface vegetation can vary considerably due to differences in: (1) the photosynthetic pathway employed by plants (C_3, C_4 or CAM); (2) factors that influence photosynthetic rate or the rate of CO_2

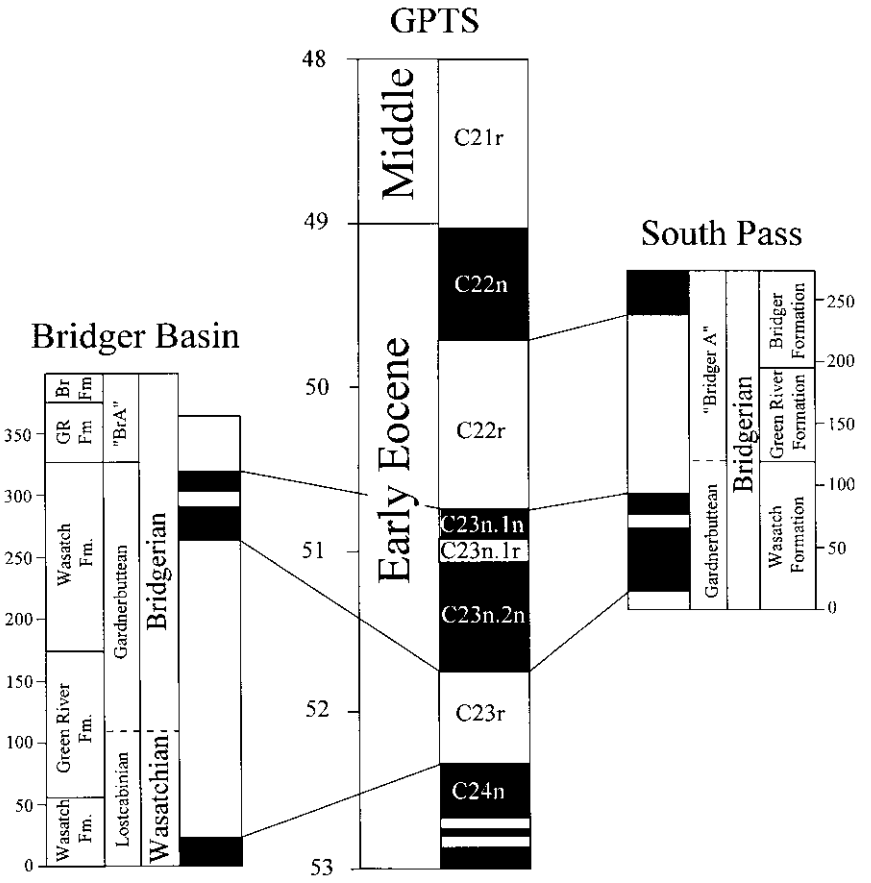

Fig. 5. Correlation of the South Pass section studied here and the Bridger Basin section from Clyde et al. (1997) to the GPTS (Cande and Kent, 1995). Notice the short reversed zone in both sections that correlates precisely with Chron C23n.1r. A radiometric age of 47.96 ± 0.13 Ma that lies about 150 m above the top of the South Pass section also supports this correlation (Murphey et al., 1999).

diffusion into plants, such as water availability, light levels, or temperature (see review by Ehleringer and Monson, 1993); and (3) fluctuations in the $\delta^{13}C$ of atmospheric CO_2 related to shifts in the global carbon cycle (Marino and McElroy, 1991). Several lines of evidence further constrain interpretations of carbon isotope records from Paleogene paleosols. For example, paleontological and isotopic evidence suggests that C_4 plants were not abundant (and may not yet have evolved) prior to the Miocene (Ehleringer and Monson, 1993; Cerling et al., 1997), and CAM plants are relatively rare, so Paleogene plant communities are thought to have been dominated by C_3 plants. In addition, carbon isotope records from fossil marine plankton preserve a relatively detailed record of long-term changes in the oceanic carbon isotope budget that can serve as a global backdrop against which local continental records can be compared (Koch et al., 1992; Grocke et al., 1999).

The $\delta^{18}O$ of soil carbonate is controlled by the $\delta^{18}O$ of soil water and temperature-dependent fractionation of oxygen isotopes during mineral formation (Friedman and O'Neil, 1977). At depths >1 m in a soil profile, monthly averages for soil and air temperature are similar, and the $\delta^{18}O$ of soil water is relatively invariant and closest in composition to meteoric water (Amundson, 1989; Brady, 1990; Hsieh et al., 1998). The $\delta^{18}O$ of modern, deeply formed soil

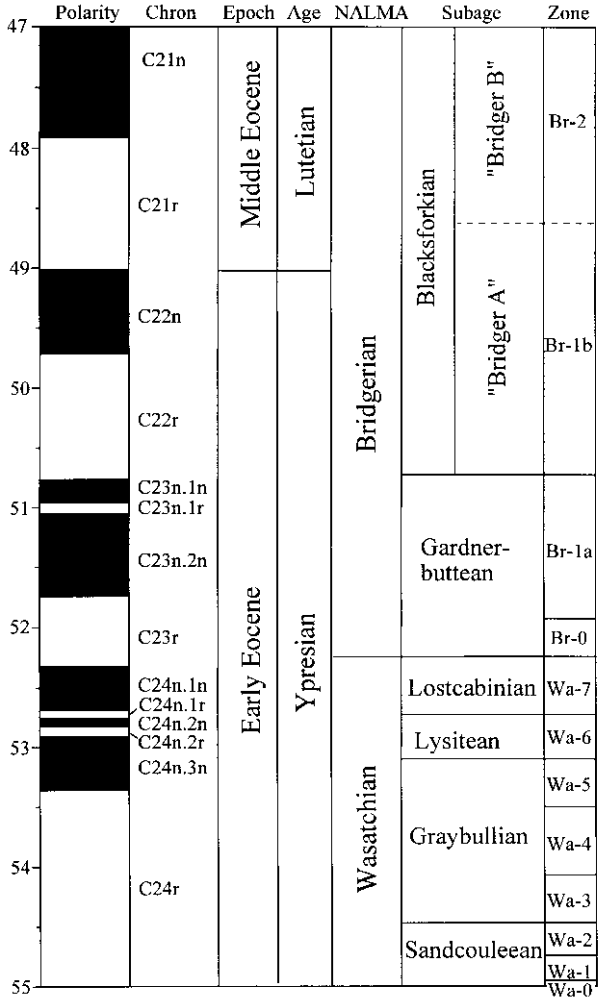

Fig. 6. Geochronology of the Wasatchian/Bridgerian framework based on the correlation shown in Fig. 5. The Wasatchian/Bridgerian boundary lies in Chron C23r in the middle of the early Eocene rather than near the early/middle Eocene boundary as previously assumed. This correlation makes the Bridgerian NALMA (especially the Gardnerbuttean subage) significantly longer than previously thought and shortens the duration of the Lostcabinian subage of the Wasatchian NALMA. The age of ~55.0 Ma for the base of the Wasatchian is based on Wing et al. (2000).

carbonate is strongly correlated to that of meteoric water, but these carbonates are typically ^{18}O-enriched by 2–10‰ relative to calcite in equilibrium with meteoric water, most likely owing to evaporative enrichment of soil water (Cerling and Quade, 1993; Liu et al., 1996).

The δ^{18}O of paleosol carbonates may shift in response to climate change through the direct effects of temperature on oxygen isotope fractionation and the effects of rainfall abundance on evaporative water loss from soils. Climate also influences the δ^{18}O of the water supplied to soils as rain and snow (Dansgaard, 1964). In temperate and boreal regions, mean annual temperature and mean annual meteoric water δ^{18}O values show a strong, positive correlation, with a slope of ~6.0‰ per °C (Rozanski et al., 1993). Individual mid- to high-latitude sites also exhibit a seasonal relationship between the δ^{18}O of meteoric

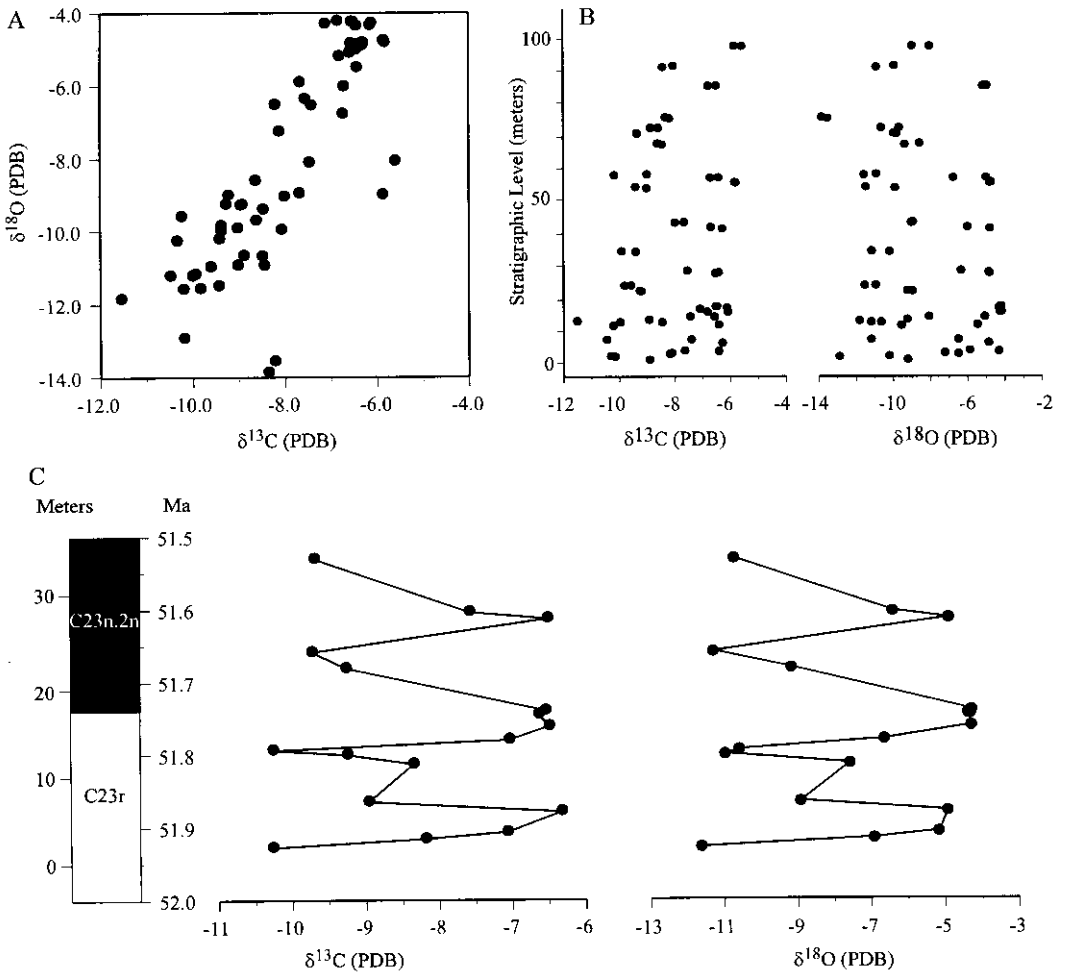

Fig. 7. Carbon and oxygen isotope compositions of paleosol carbonates from the Wasatch Formation at South Pass. (A) Bivariate plot of $\delta^{13}C$ and $\delta^{18}O$ of individual nodules showing large degree of variation and a strong positive correlation. (B) Stratigraphic plot of $\delta^{13}C$ and $\delta^{18}O$ of paleosol nodules showing high intersite variation but little to no secular trend. (C) Average $\delta^{13}C$ and $\delta^{18}O$ of paleosol nodules for a sequence of sites in the lower part of the section where sampling was most continuous. The duration between the lowest and highest levels shown here is 397,000 years based on the correlation presented in this paper. Assuming four cycles are represented, the cycles would have an average duration of 99,000 years suggesting that they may be modulated by variations in orbital eccentricity.

water and temperature, with lower values in cold months. These average and seasonal relationships result from ^{16}O-enrichment during evaporation from warm oceans, loss of ^{18}O-enriched water via rainout during vapor transport to cooler regions, and equilibration of falling droplets with local water vapor (Gat, 1996). In tropical and subtropical regions, seasonal variations are smaller, and the average $\delta^{18}O$ value is more strongly related to the amount of precipitation, with lower values in areas with greater rainfall (Rozanski et al., 1993). While the controls on paleosol carbonate $\delta^{18}O$ values are complex, it is clear that large changes in $\delta^{18}O$ values indicate major changes in environmental conditions (e.g. Cerling and Quade, 1993; Koch et al., 1995; Amundson et al., 1996).

5.2. Results

Paleosol carbonates from South Pass show considerable temporal variation in carbon and oxygen

isotope composition (Fig. 7A and B, Appendix A). Within-site variability is low. Average intra-nodule differences are 0.4‰ for $\delta^{13}C$ and 0.9‰ for $\delta^{18}O$, and average differences between nodules from the same level are 0.7‰ for $\delta^{13}C$ and 1.2‰ for $\delta^{18}O$. In contrast, through time, paleosol carbonates show in-phase cyclic variations of ~6‰ for $\delta^{18}O$ and ~3.5‰ for $\delta^{13}C$ (Fig. 7C). The cyclic pattern is especially well developed in the lowermost 35 m of the composite section, where the sampling is most continuous. Additional variations occur throughout the upper portion of the section, but lower sampling resolution renders these cycles poorly constrained.

The magnetostratigraphic correlation provides a chronostratigraphic reference with which to calibrate these isotopic cycles in absolute time. At the base of the section, where the cycles are constrained best, there are four apparent cycles between 2.0 and 34.1 m (Fig. 7C). Using the average sediment accumulation rate calculated for Chron C23n in the section (80.82 m/My), the four cycles combined are estimated to represent an interval of 397,000 years. Taking into account the errors associated with placement of the upper and lower boundaries of Chron C23n in the section, it is unlikely that these four cycles represent less than 385,00 years or more than 417,000 years. The spacing of the cycles at approximately 100,000 years suggests the possibility that they represent an environmental or geological response to variations in orbital eccentricity, an issue discussed in greater detail below.

6. Paleoclimatic and biotic implications

6.1. The Cenozoic Global Climatic Optimum

Establishing the synchroneity of geological events in the marine and continental record is a key criterion for evaluating causal relationships and assessing the integration of the earth system. The geological time scale is the standard by which synchrony is most easily tested and is thus invaluable in our continuing efforts to document earth system history. Magnetostratigraphic results presented here suggest that the Wasatchian/Bridgerian boundary correlates to Chron C23r. The most recent compilation of Cenozoic global temperatures as recorded by the oxygen isotope composition of benthic foraminifera indicates that the warmest interval of the entire Cenozoic (CGCO) also begins in Chron C23r (Zachos et al., 1994, personal communication; Fig. 8). This finding places the Wasatchian/Bridgerian boundary in a growing pool of land mammal age boundaries (e.g. Lancian/Puercan and Clarkforkian/Wasatchian) that coincide with global climatic changes and supports the view of a strong coupling between the earth's biotic and climatic systems. Although not all global climatic events coincide with significant mammalian turnover (Alroy, 1995; Prothero, 1999), it is very clear that climate can be an important driving force in regulating intercontinental dispersal (Woodburne and Swisher, 1995). In the case of the Wasatchian/Bridgerian boundary, the mammalian turnover and coincident global climatic changes are more gradual and less extreme than the changes that occurred at the preceding Clarkforkian/Wasatchian boundary (Clyde and Gingerich, 1998). However, the climate at the Wasatchian/Bridgerian boundary represents the culmination of an approximately 8 Ma period of global warming (Zachos et al., 1994, however see Wing et al., 2000 also) and this had several significant effects on continental biotas. There is a general increase in the diversity of perissodactyls, artiodactyls, and rodents and an accompanying decrease in the diversity of condylarths going from the Wasatchian into the Bridgerian (Gunnell and Bartels, 1994). Bridgerian primate faunas during this temperature maximum are quite different from those in the Wasatchian with only 22% of the genera being shared between the two land mammal ages (Gunnell, 1997). Reptilian diversity and geographic ranges were at their Cenozoic maximum during this period (Hutchison, 1982; Markwick, 1994) and tropical closed habitat ecosystems were widespread at mid to high latitudes (MacGinitie et al., 1974; Wilf, 2000). By the end of the Bridgerian, global climate had begun its long deterioration into the ice-house and North America had seen its last tropical biota of the Cenozoic (Stucky, 1990).

6.2. Isotope oscillations

The best resolved of the large isotopic cycles in the South Pass section are approximately 100,000 years in duration, indicating that these cycles may be paced by

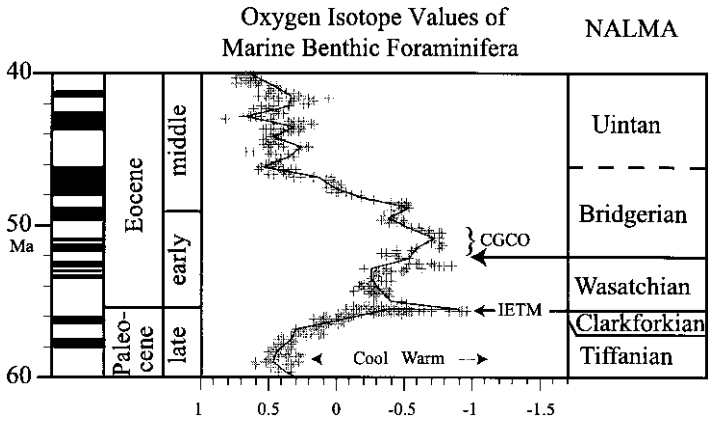

Fig. 8. Oxygen isotope record of benthic foraminifera from deep sea sites showing: (1) the coincidence of the Clarkforkian/Wasatchian NALMA boundary to a short-term negative excursion representing an abrupt global warming event (IETM); and (2) the coincidence of the Wasatchian/Bridgerian NALMA boundary to the beginning of the long-term Cenozoic warming peak known as the Cenozoic Global Climate Optimum (CGCO). Isotope data are from Zachos et al. (1994) and Zachos (personal communication). Calibration of the Geomagnetic Polarity Time Scale shown at left is from Cande and Kent (1995).

variations in orbital eccentricity. Our sampling resolution is presently too coarse to allow us to search for additional cycles nested within these 100,000 year cycles, which would supply an important test of their origin by orbital forcing.

There are several potential explanations for the large oscillations in isotope values. The $\delta^{18}O$ values of paleosol carbonates are tracking some combination of change in soil temperature and change in the $\delta^{18}O$ of soil water. We consider it unlikely that the 6‰ oscillations in carbonate $\delta^{18}O$ could result solely from change in temperature. Assuming the $\delta^{18}O$ of soil water was constant, the magnitude of the required temperature change (~25°C assuming the fractionation relationship of Friedman and O'Neil (1977)) is quite large. In addition, the positive correlation between mean annual temperature and the $\delta^{18}O$ of precipitation (Dansgaard, 1964) will oppose the negative correlation between temperature and calcite $\delta^{18}O$ produced by effects of temperature on the fractionation factor. As a consequence of these antagonistic effects, it would take an even larger temperature change to explain a 6‰ shift in carbonate $\delta^{18}O$. Consequently, we must consider alternative mechanisms that have their primary impact on the $\delta^{18}O$ of soil water.

At least three such mechanisms are possible. (1) Because precipitation in continental regions exhibits strong seasonal variations, shifts in the seasonal distribution of precipitation can shift the annually integrated $\delta^{18}O$ of soil water. For example, Plummer (1993) invoked this mechanism to explain shifts in the composition of the Florida aquifer between glacial and modern times. (2) Precipitation derived from different source regions can be isotopically distinct, due to differences in temperature at the site of vapor formation or differences in extent of rainout along the path of vapor transport (Gat 1996). Amundson et al. (1996) posited that a shift in the $\delta^{18}O$ of soil carbonates in Wyoming from glacial to Recent times could be explained by an increased component of Pacific moisture in the Recent, relative to moisture from the Gulf of Mexico. A similar mechanism could contribute to isotopic oscillations in the Eocene. (3) Finally, the $\delta^{18}O$ oscillations may reflect changes in the moisture balance of soils. Given the effects of evaporation on soil water $\delta^{18}O$ values, we would expect low carbonate $\delta^{18}O$ values to represent wetter soils, whereas higher values would indicate drier soils.

All three of these mechanisms might vary in intensity with orbital changes in insolation. There is growing evidence that orbitally driven changes in insolation have changed the intensity of monsoonal conditions over Quaternary time scales. Significant effects on the seasonality of precipitation, soil moisture state, lake level, and vegetation have been

recorded in sedimentological and pedogenic isotope records (Webb et al., 1993; Kutzbach et al., 1996; Wang and Follmer, 1998; Fang et al., 1999). Eocene wet–dry phases are known from the central Green River basin, with periodic drying of paleolake Gosuite (Buchheim, 1994). Orbitally phased changes have been detected in Eocene lacustrine oil shales from the basin as well (Fischer and Roberts, 1991; Roehler, 1993). Computer simulations of Eocene climates have revealed that orbitally driven variations in insolation can have a major impact on climate in western North America (Sloan and Morrill, 1998), though the effects on monsoonal vapor transport have yet to be investigated. Thus while the proximate cause for the large shifts in paleosol carbonate $\delta^{18}O$ values requires further study, orbitally driven changes in vapor transport and moisture balance of the paleolake basin are plausible.

The nearly 4‰ cycles in the $\delta^{13}C$ of paleosol carbonates are harder to explain. The single large $\delta^{13}C$ shift at the IETM has been attributed to a massive release of ^{13}C-depleted methane clathrates from the ocean floor, which labeled both marine and continental carbon reservoirs (Dickens et al., 1997). We might posit that orbitally driven shifts in insolation somehow triggered a series of methane releases later in the early Eocene. A possible trigger could be orbitally driven changes in the temperature of deep bottom waters beyond some critical threshold that leads to clathrate destabilization. If this mechanism is correct, then these oscillations should be a global phenomenon. There is some suggestion from marine stable isotope records that additional short-term negative excursions are present during this period (Thomas and Zachos, 1999). Unfortunately, this section of the marine record has not been examined at high enough resolution to firmly establish the presence of such shifts, much less whether or not they occur on orbital time scales. In addition, it is unclear that the marine clathrate reservoir could regenerate enough methane in just 100,000 years to explain the large $\delta^{13}C$ cycles present in South Pass soil carbonates. Finally, unlike the situation at the IETM, where paleosol carbonate $\delta^{13}C$ values drop to extremely low values (-12 to -15‰), an expected response to a large injection of ^{13}C-depleted methane into earth surface carbon reservoirs, the cycles in the South Pass paleosol carbonates do not oscillate to unusually low values (-11 to -9‰). Assuming the same isotopic offsets among surficial carbon reservoirs as operate today (Koch et al., 1995), these low values are wholly consistent with the values in coeval planktonic foraminifera. Rather, it is the $\delta^{13}C$ value for the high end of these cycles (-7 to -6‰) that is unusual and requires explanation.

There are at least two local phenomena that might explain cyclic variations from 'typical' to unusually high $\delta^{13}C$ values. First, even if we assume that Eocene vegetation consisted only of C_3 plants, it is well known that C_3 plants exhibit large, consistent differences in $\delta^{13}C$ related to changes in moisture availability, light level, and other environmental factors that influence photosynthetic rate (Ehleringer and Monson, 1993). Ecosystem-level differences in the $\delta^{13}C$ of C_3 vegetation between arid regions and wetter regions are of the magnitude of 3 to 6‰, with higher values under more arid climates (Tieszen, 1994). Thus extreme, basin-scale wet–dry cycles could explain positively correlated variations in both carbon and oxygen isotopes in paleosol carbonates. One difficulty with this hypothesis is the unlikelihood of generating soil carbonates in the extremely wet environments that would be required to produce the full range of $\delta^{13}C$ values observed here.

An alternate explanation for the $\delta^{13}C$ oscillations, as well as the unusually high $\delta^{13}C$ values in some soils, is that C_4 plants were present in the Eocene of Wyoming. Quade et al. (1994) evaluated the magnitudes of the different factors influencing the $\delta^{13}C$ of soil carbonates (variations in plants or soil productivity, temperature effects on fractionation, etc.), and argued that soil carbonate $\delta^{13}C$ values higher than ~ -8‰ are extremely unlikely in 100% C_3 ecosystems. Using the same conservative criterion, it is possible that C_4 plants were migrating into and out of these basin-margin habitats in-phase with climatic cycles indicated by the oxygen isotope record. No C_4 plant macrofossils have been discovered in deposits older than late Miocene, and prior isotopic evidence from soil carbonates and mammal tooth enamel largely point to the late Miocene for the expansion of C_4 plants into global ecosystems (Cerling et al., 1997, though see Morgan et al., 1994 for a dissenting view). If our alternate interpretation of South Pass carbonate $\delta^{13}C$ values is correct, C_4 plants were present much earlier, but limited to water-stressed,

perhaps hyper-saline environments along the margins of ancient lakes and playas.

A final interpretation is that the isotopic oscillations at South Pass record climatically controlled differences in the extent of pedogenesis. Perhaps during cool/dry intervals, soil carbonates in weakly developed paleosols incorporate a greater fraction of detrital carbonate from the soil parent material, whereas under warmer/wetter conditions, detrital carbonate is entirely removed from the soil profile by leaching. Detrital carbonates in this region would most likely be derived from the Paleozoic marine carbonates being unroofed along adjacent highlands. These carbonates tend to have $\delta^{13}C$ and $\delta^{18}O$ values much higher than those for typical soil carbonates forming in temperate/subtropical C_3 ecosystems. For example, the Mississippian aged Madison Limestone has average $\delta^{13}C$ and $\delta^{18}O$ values of $+3‰$ and $-1‰$, respectively (Budai and Lohmann, 1984). Thus, changes in the degree of incorporation of Paleozoic detrital carbonate into Eocene paleosol carbonates could induce synchronous, positively correlated changes in carbon and oxygen isotopes.

We plan to investigate these alternate hypotheses through future research. We will collect paleosol carbonates at greater stratigraphic resolution to search for sub-cycles that might bolster our interpretation that the 100,000 year cycles are orbitally forced, and allow us to identify clearer cycles higher in the stratigraphic section. In the process, we will conduct more exhaustive field and laboratory analyses of paleosol properties to explore whether or not isotopic cycles are tied to paleosol maturity and development. Finally, we will test the provocative hypothesis that C_4 plants were present in the Eocene of Wyoming through isotopic analysis of mammals from the same paleosols that produce unusually high soil carbonate $\delta^{13}C$ values. If these high values reflect the presence of C_4 plants, rather than a pedogenic process that leads to spuriously high values (such as the incorporation of more detrital carbonate under conditions of low soil productivity), then mammals feeding on these C_4 plants should have unusually high $\delta^{13}C$ values in their tooth enamel. Of course, recovery of plant fossils might also resolve this issue, but upland sedimentary environments like those at South Pass rarely preserve good plant fossils.

6.3. Anachronism

Recent paleontological surveys across the Wasatchian/Bridgerian boundary from several areas in the greater Green River Basin have indicated the possibility that faunas preserved in basin-margin settings may differ significantly from coeval basin-center faunas (Gunnell and Bartels, 2001). This hypothesis is strongly supported by the results presented here. The stratigraphic order of lithological, biostratigraphic and magnetostratigraphic datums coincides precisely between the Bridger Basin, which lies in the west-central greater Green River Basin (Fig. 1A; Clyde et al., 1997), and the South Pass area studied here. This suggests that each of these transitions is essentially isochronous between sections (at least at the time scale of polarity reversals). First and last appearance events for certain taxa, however, seem to differ significantly in these two sections. For instance, the perissodactyl taxa *Hyracotherium* and *Orohippus*, often thought of as a classic example of an anagenetic ancestor-descendent pair due to similar morphologies and non-overlapping stratigraphic ranges in basin-center faunas, are found to overlap in the basin-margin section at South Pass (Fig. 9). Several other examples of anachronistic biostratigraphic datums and compositional disparity between basin-margin and basin-center faunas have been documented from the greater Green River Basin, suggesting there may have been considerable ecological heterogeneity across this broad basin in the Eocene (Gunnell and Bartels, 2001). Results presented here argue that these differences are not an artifact of diachronous lithological boundaries. It is also unlikely that the differences are due to excessive time-averaging along the basin-margin since all of the lithological and magnetostratigraphic datums that are preserved in the basin-center are also preserved on this margin. In addition, the taxa in question have been recorded in several different paleosol horizons in the South Pass section suggesting that time-averaging could not be the sole reason for the observed pattern.

One explanation for the observed disparity between biostratigraphic and compositional characteristics of basin-margin faunas compared to coeval basin-center faunas includes the potential existence of refuge habitats along these marginal settings. It is almost certain that the Green River Basin in the Eocene had a much wider variety of habitats than it does today and

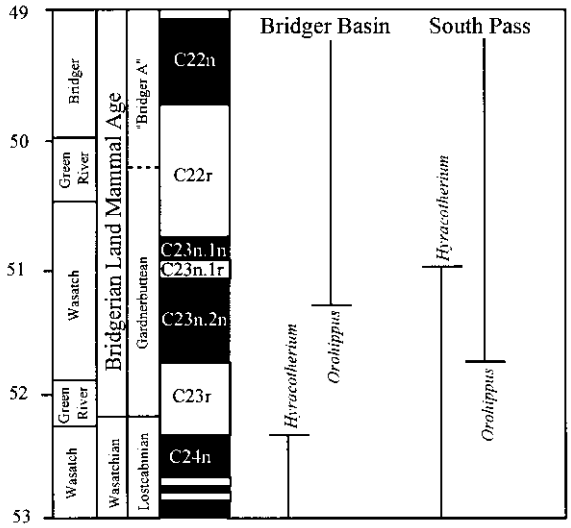

Fig. 9. An example of diachronous biostratigraphic datums between the upland South Pass section and the more central Bridger Basin section from Clyde et al. (1997). The stratigraphic ranges of *Hyracotherium* and *Orohippus* overlap at South Pass whereas their ranges do not overlap in the Bridger Basin section.

thus it may not be surprising to see variation in the stratigraphic distribution of certain habitat-specific taxa. It is important to note, however, that even though several individual taxa seem to exhibit anachronistic biostratigraphic datums between sections, the boundaries between faunal zones (e.g. between the Gardnerbuttean and Blacksforkian subages) are still clearly identifiable and seem to be essentially synchronous between sections. This is true because the index taxa (usually genera) tend to be large, broadly distributed generalists (e.g. brontotheres) that exhibit local differences in relative abundance but are characterized by less taxonomic turnover than their specialist cohorts (e.g omomyids).

The seeming isochrony of lithological transitions across the greater Green River basin is surprising given its size and complexity. Paleolake Gosuite, the most important sedimentary architect in this basin, seems to have experienced dramatic changes in lake level over very short periods of time suggesting it may have been quite sensitive to extrabasinal phenomena like climatic change. Although faunal sampling is not yet resolved enough to assess the biotic impact of these local, short-term environmental fluctuations, it is clear that mammalian faunas in this region experienced significant reorganization coincident with the global changes in climate at the CGCO. Continued sampling of the excellent record of Eocene environmental and biotic change preserved in the greater Green River Basin should provide the opportunity to evaluate the local response to the global climatic changes that occurred around the CGCO.

7. Conclusions

Magnetostratigraphic and isotopic results presented here for South Pass have several important implications for constraining faunal and climatic changes in North America during the early Eocene:

1. New magnetostratigraphic information from South Pass suggests that the Wasatchian/Bridgerian boundary correlates to Chron C23r at about 52 Ma on the most recent GPTS.
2. This new correlation indicates that the Wasatchian/Bridgerian boundary correlates with the onset of the CGCO (Cenozoic Global Climatic Optimum) which represents the warmest interval of the entire Cenozoic.

3. Carbon and oxygen isotope composition of paleosol carbonates exhibit high amplitude cycles (~6‰ for oxygen and ~3.5‰ for oxygen) that are estimated to be 100,000 years in duration suggesting a potential link with variations in orbital eccentricity.
4. Intrabasinal correlations suggest that lithological and biostratigraphic boundaries are isochronous across the basin but that particular taxa seem to exhibit significantly different first or last appearances in basin-margin sections like South Pass compared to coeval basin-center sections. Basin-margin areas may act as long-term refugia for ecologically sensitive taxa.

Acknowledgements

This work was funded by NSF grant EAR-9619908 (to WSB) and a grant from the University of Michigan Sokal Endowment (to GFG and WCC). We thank J. Zachos for sharing unpublished data. M. Woodburn and P. Gingerich provided helpful reviews of the manuscript.

Appendix A

Carbon and oxygen isotope compositions of paleosol carbonate nodules from the Wasatch Formtion at South Pass. Isotopic values are relative to the PDB standard. Ages for each level are estimated using the base of Chron C23n.2n (following the correlation shown in Fig. 5; Cande and Kent, 1995) and an average sediment accumulation rate for C23n (80.83 m/My).

Sample	Section	Composite level (m)	Age (Ma)	Sample $\delta^{13}C$	Sample $\delta^{18}O$	Nodule average $\delta^{13}C$	Nodule average $\delta^{18}O$	Level average $\delta^{13}C$	Level average $\delta^{18}O$
SP-PM-98001A-1	98-PM-1	0.90	51.94	−8.86	−9.28	−8.94	−9.28	−8.94	−9.28
SP-PM-98001A-2				−9.02	−9.28				
SP-PM-98002A-1	98-PM-1	2.05	51.93	−10.35	−10.06	−10.34	−10.27	−10.26	−11.61
SP-PM-98002A-2				−10.33	−10.49				
SP-PM-98002B-1				−10.30	−13.07	−10.19	−12.94		
SP-PM-98002B-2				−10.08	−12.81				
SP-PM-98003A-1	98-PM-1	3.00	51.92	−7.56	−6.88	−8.14	−7.27	−8.18	−6.90
SP-PM-98003A-2				−8.72	−7.66				
SP-PM-98003B-1				−7.23	−5.20	−8.22	−6.53		
SP-PM-98003B-2				−9.22	−7.87				
SP-PM-98004A-1	98-PM-1	3.75	51.91	−7.60	−4.88	−7.68	−5.93	−7.07	−5.15
SP-PM-98004A-2				−7.77	−6.97				
SP-PM-98004B-1				−6.49	−4.15	−6.46	−4.38		
SP-PM-98004B-3				−6.42	−4.61				
SP-PM-98006A-1	98-PM-1	6.05	51.88	−6.36	−3.75	−6.33	−4.91	−6.33	−4.91
SP-PM-98006A-2				−6.75	−5.37				
SP-PM-98006A-3				−5.87	−5.63				
SP-PM-98007A-1	98-PM-1	7.15	51.86	−9.84	−10.68	−10.49	−11.23	−8.96	−8.90
SP-PM-98007A-2				−12.02	−10.56				
SP-PM-98007A-3				−9.60	−12.45				
SP-PM-98007B-1				−7.67	−7.30	−7.44	−6.56		
SP-PM-98007B-2				−7.20	−5.82				
SP-PM-98008A-1	98-PM-1	11.35	51.81	−10.54	−9.66	−10.25	−9.61	−8.35	−7.57
SP-PM-98008A-2				−9.96	−9.56				
SP-PM-98008B-1				−6.61	−6.08	−6.44	−5.52		
SP-PM-98008B-2				−6.28	−4.97				
SP-PM-98009A-1	98-PM-1	12.37	51.80	−9.92	−11.01	−10.01	−11.23	−9.25	−10.96
SP-PM-98009A-2				−10.09	−11.44				

(*continued*)

Sample	Section	Composite level (m)	Age (Ma)	Sample $\delta^{13}C$	Sample $\delta^{18}O$	Nodule average $\delta^{13}C$	Nodule average $\delta^{18}O$	Level average $\delta^{13}C$	Level average $\delta^{18}O$
SP-PM-98009B-1				−8.49	−10.69	−8.49	−10.69		
SP-PM-98010A-1	98-PM-1	12.87	51.79	−11.50	−11.89	−11.55	−11.86	−10.26	−10.58
SP-PM-98010A-2				−11.60	−11.83				
SP-PM-98010B-1				−9.33	−10.22	−8.97	−9.29		
SP-PM-98010B-2				−8.61	−8.37				
SP-PM-98011A-1	98-PM-1	14.00	51.78	−6.85	−5.61	−6.60	−5.12	−7.04	−6.62
SP-PM-98011A-3				−6.36	−4.63				
SP-PM-98011B-1				−7.48	−8.13	−7.48	−8.13		
SP-PM-98012A-1	98-PM-1	15.50	51.76	−6.15	−4.39	−6.13	−4.30	−6.50	−4.27
SP-PM-98012A-2				−6.10	−4.22				
SP-PM-98012B-1				−6.59	−4.27	−6.87	−4.24		
SP-PM-98012B-2				−7.14	−4.21				
SP-PM-98013A-1	98-PM-1	16.80	51.75	−6.17	−4.38	−6.15	−4.36	−6.64	−4.34
SP-PM-98013A-2				−6.14	−4.34				
SP-PM-98013B-1				−7.14	−4.39	−7.13	−4.32		
SP-PM-98013B-2				−7.12	−4.25				
SP-PM-98014A-1	98-PM-1	17.25	51.74	−6.67	−4.33	−6.52	−4.28	−6.54	−4.27
SP-PM-98014A-2				−6.37	−4.22				
SP-PM-98014B-1				−6.71	−4.12	−6.56	−4.26		
SP-PM-98014B-2				−6.41	−4.40				
SP-PM-98015A-1	98-PM-2	28.25	51.60	−7.42	−6.04	−7.58	−6.38	−7.58	−6.38
SP-PM-98015A-2				−7.74	−6.73				
SP-PM-98016A-1	98-PM-3	27.50	51.61	−6.10	−4.37	−6.58	−4.86	−6.51	−4.87
SP-PM-98016A-2				−7.06	−5.35				
SP-PM-98016B-1				−6.25	−4.38	−6.45	−4.89		
SP-PM-98016B-2				−6.65	−5.40				
SP-PM-98017A-1	98-PM-2	22.00	51.68	−9.02	−8.78	−9.24	−9.02	−9.26	−9.15
SP-PM-98017A-2				−9.46	−9.26				
SP-PM-98017B-2				−9.29	−9.18	−9.29	−9.27		
SP-PM-98017B-3				−9.29	−9.37				
SP-PM-98018A-1	98-PM-2	23.80	51.66	−9.38	−10.35	−9.61	−10.98	−9.73	−11.28
SP-PM-98018A-2				−9.84	−11.61				
SP-PM-98018B-1				−9.74	−11.26	−9.84	−11.57		
SP-PM-98018B-2				−9.94	−11.88				
SP-PM-98019A-2	98-PM-3	34.10	51.53	−9.30	−10.36	−9.43	−10.22	−9.69	−10.70
SP-PM-98019A-3				−9.56	−10.08				
SP-PM-98019B-1				−9.78	−10.61	−9.95	−11.18		
SP-PM-98019B-2				−10.40	−11.90				
SP-PM-98019B-3				−9.67	−11.03				
SP-PM-98020A-1	98-PM-3	41.10	51.44	−5.95	−4.42	−6.32	−4.84	−6.52	−5.44
SP-PM-98020A-3				−6.68	−5.25				
SP-PM-98020B-1				−7.71	−7.08	−6.73	−6.04		
SP-PM-98020B-2				−5.75	−5.01				
SP-PM-98021A-2	98-PM-3	42.90	51.42	−8.31	−9.23	−8.02	−9.06	−7.86	−9.02
SP-PM-98021A-3				−7.73	−8.89				
SP-PM-98021B-1				−7.69	−8.97	−7.69	−8.97		

(*continued*)

Sample	Section	Composite level (m)	Age (Ma)	Sample $\delta^{13}C$	Sample $\delta^{18}O$	Nodule average $\delta^{13}C$	Nodule average $\delta^{18}O$	Level average $\delta^{13}C$	Level average $\delta^{18}O$
SP-PM-98023A-1	98-PM-4	53.95	51.29	−10.02	−11.21	−9.44	−11.50	−9.24	−10.72
SP-PM-98023A-3				−8.86	−11.79				
SP-PM-98023B-1				−9.67	−8.84	−9.04	−9.93		
SP-PM-98023B-2				−8.41	−11.03				
SP-PM-98024A-1	98-PM-4	55.45	51.27	−5.72	−4.46	−5.87	−4.78	−5.85	−4.80
SP-PM-98024A-2				−6.01	−5.10				
SP-PM-98024B-1				−5.77	−4.59	−5.84	−4.83		
SP-PM-98024B-2				−5.91	−5.08				
SP-PM-98025A-1	98-PM-4	56.80	51.25	−6.53	−5.47	−6.75	−6.79	−6.60	−5.91
SP-PM-98025A-2				−6.96	−8.11				
SP-PM-98025B-1				−6.35	−4.71	−6.46	−5.03		
SP-PM-98025B-2				−6.56	−5.35				
SP-PM-98026A-1	98-PM-4	57.95	51.24	−9.35	−11.54	−9.03	−10.94	−9.61	−11.26
SP-PM-98026A-2				−8.70	−10.34				
SP-PM-98026B-1				−10.03	−11.47	−10.20	−11.59		
SP-PM-98026B-2				−10.37	−11.71				
SP-PM-98029A-1	98-PM-4	67.00	51.12	−8.45	−9.45	−8.48	−9.41	−8.57	−9.01
SP-PM-98029A-2				−8.51	−9.37				
SP-PM-98029B-1				−8.70	−8.42	−8.65	−8.62		
SP-PM-98029B-2				−8.60	−8.81				
SP-PM-98030A-1	98-PM-4	70.40	51.08	−9.12	−9.37	−9.39	−9.86	−9.39	−9.93
SP-PM-98030A-2				−9.65	−10.35				
SP-PM-98030B-1				−9.26	−9.79	−9.39	−10.00		
SP-PM-98030B-2				−9.52	−10.21				
SP-PM-98031A-1	98-PM-4	72.20	51.06	−8.69	−10.26	−8.89	−10.68	−8.76	−10.20
SP-PM-98031A-2				−9.09	−11.10				
SP-PM-98031B-1				−8.47	−9.09	−8.63	−9.72		
SP-PM-98031B-2				−8.79	−10.35				
SP-PM-98032A-1	98-PM-4	75.10	51.02	−8.32	−12.30	−8.22	−13.57	−8.29	−13.73
SP-PM-98032A-2				−8.13	−14.84				
SP-PM-98032B-1				−8.51	−14.24	−8.37	−13.88		
SP-PM-98032B-2				−8.22	−13.52				
SP-PM-98033A-1	98-PM-4	85.10	50.90	−6.74	−4.80	−6.83	−5.21	−6.69	−5.11
SP-PM-98033A-2				−6.92	−5.62				
SP-PM-98033B-1				−6.38	−4.53	−6.54	−5.00		
SP-PM-98033B-2				−6.71	−5.48				
SP-PM-98034A-1	98-PM-4	91.20	50.83	−8.01	−9.77	−8.08	−9.98	−8.27	−10.46
SP-PM-98034A-2				−8.15	−10.19				
SP-PM-98034B-1				−8.53	−10.56	−8.45	−10.95		
SP-PM-98034B-2				−8.38	−11.33				
SP-PM-98043A-1	98-PM-6	97.35	50.75	−6.02	−7.26	−5.88	−9.01	−5.74	−8.55
SP-PM-98043A-2				−5.74	−10.77				
SP-PM-98043B-1				−5.59	−7.96	−5.61	−8.09		
SP-PM-98043B-2				−5.63	−8.21				

References

Alroy, J., 1995. Does climate or competition control mammalian diversity. Journal of Vertebrate Paleontology 15, 16.

Alroy, J., 1999. The fossil record of North American mammals: evidence for a Paleocene evolutionary radiation. Systematic Biology 48, 107–118.

Amundson, R., 1989. The use of stable isotopes in assessing the effect of agriculture on arid and semi-arid soils. In: Rundel, P.W., Ehleringer, J.R., Nagy, K.A. (Eds.), Stable Isotopes in Ecological Research. Springer, New York, pp. 318–341.

Amundson, R., Chadwick, O., Kendall, C., Wang, Y., Deniro, M., 1996. Isotopic evidence for shift in atmospheric circulation patterns during the late Quaternary in mid-North America. Geology 24, 23–26.

Aubry, M.-P., Lucas, S., Berggren, W.A. (Eds.), 1998. Late Paleocene–early Eocene Climatic and Biotic Evolution Columbia University Press, New York.

Berggren, W.A., Lucas, S., Aubry, M.-P., 1998. Late Paleocene–Early Eocene climatic and biotic evolution: an overview. In: Aubry, M.-P., Lucas, S.G., Berggren, W.A. (Eds.), Late Paleocene–Early Eocene Climatic and Biotic Events in the Marine and Terrestrial Records. Columbia University Press, New York, pp. 1–17.

Brady, N.C., 1990. The Nature and Properties of Soils. Macmillan, New York, 621 pp.

Buchheim, P.H., 1994. Eocene Fossil Lake, Green River Formation, Wyoming; a history of fluctuating salinity. In: Renaut, R.W., Last, W.M. (Eds.), Sedimentology and Geochemistry of Modern and Ancient Saline Lakes. Special Publication — (SEPM) Society of Sedimentary Geology, 50, pp. 239–247.

Budai, J.M., Lohmann, K.C., 1984. Burial dedolomite in the Mississippian Madison Limestone, Wyoming and Utah thrust belt. Journal of Sedimentary Petrology 54, 276–288.

Butler, R.F., Gingerich, P.D., Lindsay, E.H., 1981. Magnetic polarity stratigraphy and biostratigraphy of Paleocene and lower Eocene continental deposits, Clarks Fork Basin, Wyoming. Journal of Geology 89, 299–316.

Cande, S.C., Kent, D.V., 1995. Revised calibration of the geomagnetic polarity time scale for the Late Cretaceous and Cenozoic. Journal of Geophysical Research 100, 6093–6095.

Cerling, T., 1984. The stable isotopic composition of modern soil carbonate and its relationship to climate. Earth and Planetary Science Letters 71, 229–240.

Cerling, T.E., 1992. Use of caron isotopes in paleosols as an indicator of the P(CO2) of the paleoatmosphere. Global and Planetary Change 6, 307–314.

Cerling, T.E., Harris, J.M., MacFadden, B.J., Leakey, M.G., Quade, J., Eisenmann, V., Ehleringer, J.R., 1997. Global vegetation change through the Miocene/Pliocene boundary. Nature 389, 153–158.

Cerling, T.E., Quade, J., 1993. Stable carbon and oxygen isotopes in soil carbonates. In: Swart, P.K., Lohmann, K.C., McKenzie, J., Savin, S. (Eds.), Climate Change in Continental Isotope Records. Geophysical Monograph 78, American Geophysical Union, Washington, DC, pp. 217–231.

Cerling, T.E., Quade, J., Wang, Y., Bowman, J.R., 1989. Carbon isotopes in soils and paleosols as ecology and paleoecology indicators. Nature 341, 138–139.

Clyde, W.C., Gingerich, P.D., 1998. Mammalian community response to the latest Paleocene thermal maximum: an isotaphonomic study in the northern Bighorn Basin, Wyoming. Geology 26, 1011–1014.

Clyde, W.C., Stamatakos, J., Gingerich, P.D., 1994. Chronology of the Wasatchian Land-Mammal Age (early Eocene): magnetostratigraphic results from the McCullough Peaks section, northern Bighorn Basin, Wyoming. Journal of Geology 102, 367–377.

Clyde, W.C., Zonneveld, J.-P., Stamatakos, J., Gunnell, G.F., Bartels, W.S., 1997. Magnetostratigraphy across the Wasatchian–Bridgerian boundary (early to middle Eocene) in the western Green River Basin, Wyoming. Journal of Geology 105, 657–669.

Cope, E.D., 1873. Descriptions of new extinct reptiles from the upper Green River Eocene basin, Wyoming. Proceedings of the American Philisophical Society, 554–555.

Dansgaard, W., 1964. Stable isotopes in precipitation. Tellus 16, 436–468.

Dickens, G.D., Castillo, M.M., Walker, J.C.G., 1997. A blast of gas in the latest Paleocene: simulating first-order effects of massive dissociation of oceanic methane hydrate. Geology 25, 259–262.

Diehl, J.F., Beck Jr., M.E., Beske-Diehl, S., Jacobson, D., Hearn Jr., B.C., 1983. Paleomagnetism of the Late Cretaceous–early Tertiary north-central Montana alkalic province. Journal of Geophysical Research 88, 10,593–10,609.

Ehleringer, J.R., Monson, R.K., 1993. Evolutionary and ecological aspects of photosynthetic pathway wariation. Annual Review of Ecology and Systematics 24, 411–439.

Evanoff, E., Brand, L.R., Murphey, P.C., 1998. Bridger Formation (middle Eocene) of southwest Wyoming: widespread marker units and subdivisions of Bridger B through D. Dakoterra 5, 115–122.

Fang, X.M., Ono, Y., Fukuksawa, H., Pan, B.T., Li, J.L., Guan, D.H., Oi, K.C., Tsukamoto, S., Torii, M., Mishima, T., 1999. Asian summer monsoon instability during the past 60,000 years: magnetic susceptibility and pedogenic evidence from the western Chinese Loess Plateau. Earth and Planetary Science Letters 168, 219–232.

Fischer, A.G., Roberts, L.T., 1991. Cyclicity in the Green River Formation (lacustrine Eocene) of Wyoming. Journal of Sedimentary Petrology 61, 1146–1154.

Fisher, R.A., 1953. Dispersion on a sphere. Proceedings of the Royal Society (London) A217, 295–305.

Flynn, J.J., 1986. Correlation and geochronology of middle Eocene strata from the western United States. Palaeogeography, Palaeoclimatology, Palaeoecology 55, 335–406.

Friedman, I., O'Neil, 1977. Compilation of stable isotope fractionation factors of geochemical interest. Fleischer, M. (Ed.), Data of Geochemistry. US Geological Survey Professional Paper, 440-KK, 12 pp.

Gat, J.R., 1996. Oxygen and hydrogen isotopes in the hydrological cycle. Annual Review of Earth and Planetary Sciences 24, 225–262.

Grande, L., 1984. Paleontology of the Green River Formation, with a review of the fish fauna. Geological Survey of Wyoming Bulletin 63, 1–333.

Grocke, D.R., Hesselbo, S.P., Jenkyns, H.C., 1999. Carbon-isotope composition of lower Cretaceous fossil wood: ocean–atmosphere chemistry and relation to sea-level change. Geology 27, 155–158.

Gunnell, G.F., 1997. Wasatchian–Bridgerian (Eocene) paleoecology of the western interior of North America: changing paleoenvironments and taxonomic composition of omomyid (Tarsiiformes) primates. Journal of Human Evolution 32, 105–132.

Gunnell, G.F., Bartels, W.S., 1994. Early Bridgerian (middle Eocene) vertebrate paleontology and paleoecology of the southern Green River Basin, Wyoming. University of Wyoming Contributions to Geology 30, 57–70.

Gunnell, G.F., Bartels, W.S., 2001. Basin margins, biodiversity, evolutionary innovations, and the origin of new taxa. In: Gunnell, G.F. (Ed.), Eocene Biodiversity: Unusual Occurrences and Rarely Sampled Habitats. Plenum Press, New York (in press).

Gunnell, G.F., 1998. Mammalian fauna from the lower Bridger Formation (Bridger A, early middle Eocene) of the southern Green River Basin, Wyoming. Contributions from the Museum of Paleontology, University of Michigan, 30, pp. 83–130.

Gunnell, G.F., Yarborough, V.L., 2000. Eotitanops and Palaeosyops (Brontotheriidae, Perissodactyla) from the middle Eocene (Bridgerian), Wasatch and Bridger formations, southern Green River Basin, southwestern Wyoming. Journal of Vertebrate Paleontology 20, 349–368.

Hagen, E.S., Shuster, M.W., Furlong, K.P., 1985. Tectonic loading and subsidence of intermontane basins; Wyoming foreland province. Geology 13, 585–588.

Hsieh, J.C.C., Chadwick, O.A., Kelly, E.F., Savin, S.M., 1998. Oxygen isotopic composition of soil water: quantifying evaporation and transpiration. Geoderma 82, 262–293.

Hutchison, J.H., 1982. Turtle, crocodilian, and champsosaur diversity changes in the Cenozoic of the north-central region of western United States. Palaeogeography, Palaeoclimatology, Palaeoecology 37, 149–164.

Kirschvink, J.L., 1980. The least-squares line and plane and the analysis of paleomagnetic data. Geophysics Journal of the Royal Astronomical Society 62, 743–746.

Koch, P.L., Zachos, J.C., Dettman, D.L., 1995. Stable isotope stratigraphy and paleoclimatology of the Paleogene Bighorn Basin (Wyoming, USA). Palaeogeography, Palaeoclimatology, Palaeoecology 115, 61–90.

Koch, P.L., Zachos, J.C., Gingerich, P.D., 1992. Correlation between isotope records in marine and continental carbon reservoirs near the Palaeocene/Eocene boundary. Nature 358, 319–322.

Krishtalka, L., West, R.M., Black, C.G., Dawson, M.R., Flynn, J.J., Turnbull, W.D., Stucky, R.K., McKenna, M.C., Bown, T.M., Golz, D.J., Lilligraven, J.A., 1987. Eocene (Wasatchian through Duchesnean) biochronology of North America. In: Woodburne, M.O. (Ed.), Cenozoic Mammals of North America; Geochronology and Biostratigraphy. University of California Press, Berkeley, CA, pp. 77–117.

Kutzbach, J.E., Bonan, G., Foley, J., Harrison, S.P., 1996. Vegetation and soil feedbacks on the response of the African monsoon to orbital forcing in the early to middle Holocene. Nature 384, 623–626.

Liu, B.L., Phillips, F.M., Campbell, A.R., 1996. Stable carbon and oxygen isotopes of pedogenic carbonates, Ajo Mountains, Southern Arizona — implications for paleoenvironmental change. Palaeogeography, Palaeoclimatology, Palaeoecology 124, 233–246.

MacGinitie, H.D., Leopold, E.B., Rohrer, W.L., 1974. An early middle Eocene flora from the Yellowstone-Absaroka volcanic province, northwestern Wind River Basin, Wyoming. University of California Publications in Geological Sciences, 108, pp. 1–103.

Marino, B.D., McElroy, M.B., 1991. Isotopic composition of atmospheric CO_2 inferred from carbon in C_4 plant cellulose. Nature 349, 127–131.

Markwick, P., 1994. Equability, continentality, and Tertiary climate: the crocodilian perspective. Geology 22, 613–616.

Marsh, O.C., 1872. Preliminary description of the new Tertiary reptiles. American Journal of Science 4, 298–309.

Matthew, W.D., 1909. The Carnivora and Insectivora of the Bridger Basin, middle Eocene. Memoirs of the American Museum of Natural History 9, 291–567.

McCarroll, S.M., Flynn, J.J., Turnbull, W.D., 1996. Biostratigraphy and magnetostratigraphy of the Bridgerian-Uintan Washakie Formation, Washakie Basin, Wyoming. In: Prothero, D.R., Emry, R.J. (Eds.), The Terrestrial Eocene–Oligocene Transition in North America. Cambridge University Press, Cambridge, pp. 25–39.

McFadden, P.L., Lowes, F.J., 1981. The discrimination of mean directions drawn from Fisher distributions. Geophysics Journal of the Royal Astronomical Society 67, 19–33.

McGowran, B., 1990. Fifty million years ago. American Scientist 78, 30–39.

McGrew, P.O., 1971. early and middle Eocene faunas of the Green River basin. Contributions to Geology 10, 65–68.

Mora, C.I., Driese, S.G., Colarusso, L.A., 1996. Middle to late Paleozoic atmospheric CO_2 levels from soil carbonate organic matter. Science 271, 1105–1107.

Morgan, M.E., Kingston, J.D., Marino, B.D., 1994. Carbon isotopic evidence for the emergence of C_4 plants in the Neogene from Pakistan and Kenya. Nature 367, 162–165.

Murphey, P.C., Lester, A., Bohor, B., Robinson, P., Evanoff, E., Larson, E., 1999. $^{40}Ar/^{39}Ar$ Dating of Volcanic Ash Deposits in the Bridger Formation (middle Eocene), Southwestern Wyoming. GSA Abstracts with Programs, 31, p. A233.

Norris, R.D., Jones, L.S., Corfield, R.M., 1996. Skiing in the Eocene Uinta mountains? Isotopic evidence in the Green River Formation for snow melt and large mountains. Geology 24, 403–406.

Plummer, L.N., 1993. Stable isotope enrichment in paleowaters of the southeast Atlantic Coastal Plain, United States. Science 262, 2016–2020.

Prothero, D.R., 1999. Does climate change drive mammalian evolution. GSA Today 9, 1–7.

Quade, J., Cerling, T.E., Bowman, J., 1989. Systematic variations in the carbon and oxygen isotopic compositions of pedogenic carbonate along elevation transects in the southern Great

Basin, United States. Geological Society of America Bulletin 101, 464–475.

Quade, J., Solounias, N., Cerling, T.E., 1994. Stable isotopic evidence from paleosol carbonates and fossil teeth in Greece for forest or woodlands over the past 11 Ma. Palaeogeography, Palaeoclimatology, Palaeoecology 108, 41–53.

Quade, J., Cerling, T.E., 1995. Expansion of C_4 grasses in the late Miocene of northern Pakistan: evidence from stable isotopes in paleosols. Palaeogeography, Palaeoclimatology, Palaeoecology 115, 91–116.

Roehler, H.W., 1990. Sedimentology of freshwater lacustrine shorelines in the Eocene Scheggs Bed of the Tipton Tongue of the Green River Formation, Sand Wash Basin, Northwest Colorado. US Geological Survey Bulletin B1911, 1–12.

Roehler, H.W., 1991a. Description and correlation of Eocene rocks in stratigraphic reference sections for the Green River and Washakie basins, southwest Wyoming. US Geological Survey Professional Paper 1506, 1–83.

Roehler, H.W., 1991b. Revised stratigraphic nomenclature for the Wasatch and Green River Formations of Eocene Age, Wyoming, Utah, and Colorado. US Geological Survey Professional Paper 1506, 1–38.

Roehler, H.W., 1992a. Correlation, composition, areal distribution, and thickness of Eocene stratigraphic units, greater Green River Basin, Wyoming, Utah, and Colorado. US Geological Survey Professional Paper 1506, 1–47.

Roehler, H.W., 1992b. Godiva Rim Member — a new stratigraphic unit of the Green River Formation in southwest Wyoming and northwest Colorado. US Geological Survey Professional Paper 1506, 1–17.

Roehler, H.W., 1992c. Introduction to greater Green River Basin geology, physiography, and history of investigations. US Geological Survey Professional Paper 1506, 1–14.

Roehler, H.W., 1993. Eocene climates, depositional environments, and geography, greater Green River Basin, Wyoming, Utah, and Colorado. US Geological Survey Professional Paper 1506, 1–74.

Rozanski, K., Araguas-Araguas, L., Gonfiantini, R., 1993. Isotopic patterns in modern global precipitation. In: Swart, P.K., Lohmann, K.C., McKenzie, J., Savin, S. (Eds.), Climate Change in Continental Isotope Records. Geophysical Monograph 78American Geophysical Union, Washington, DC, pp. 1–35.

Sheriff, S.D., Shive, P.N., 1982. Unreliable paleomagnetic results from the Wilkins Peak member of the Eocene Green River Formation, Wyoming. Geophysical Research Letters 9, 723–726.

Shuster, M.W., Steidtmann, J.R., 1985. Fluvial-sandstone architecture and thrust-induced subsidence, northern Green River basin, Wyoming. In: Ethridge, Frank, G. et al. (Ed.), Recent Developments in Fluvial Sedimentology. Special Publication — Society of Economic Paleontologists and Mineralogists, 39, pp. 279–285.

Sloan, L.C., Morrill, C., 1998. Orbital forcing and Eocene continental temperatures. Palaeogeography, Palaeoclimatology, Palaeoecology 144, 21–35.

Smoot, J.P., 1983. Depositional subenvironments in an arid closed basin: the Wilkins Peak Member of the Green River Formation (Eocene), Wyoming, USA. Sedimentology 30, 801–827.

Stucky, R., 1990. Evolution of land mammal diversity in North America during the Cenozoic. Current Mammalogy 2, 375–432.

Tauxe, L., Gee, J., Gallet, Y., Pick, T., Bown, T., 1994. Magnetostratigraphy of the Willwood Formation, Bighorn Basin, Wyoming: new constraints on the location of the Paleocene/Eocene boundary. Earth and Planetary Science Letters 125, 159–172.

Thomas, E., Shackleton, N.J., 1996. The Paleocene–Eocene benthic foraminiferal extinction and stable isotope anomalies. In: Knox, R.W.O., Corfield, R.M., Dunay, R.E. (Eds.), Correlation of the early Paleogene in Northwest Europe. Geological Society [London] Special Publication 101, London, pp. 401–441.

Thomas, E., Zachos, J.C., 1999. Deep-sea faunas during the late Paleocene–early Eocene climate optimum: boredom or boredom with short periods of terror? Geological Society of America Program with Abstracts, 31, p. A122.

Tieszen, L.L., 1994. Stable isotopes on the plains: vegetation analyses and diet determinations. In: Owsley, D.W., Jantz, R.L. (Eds.), Skeletal Biology in the Great Plains. Smithsonian Institution Press, Washington, DC, pp. 261–282.

Walsh, S.L., 1996. Theoretical biochronology, the Bridgerian/Uintan boundary, and the Shoshonian subage of the Uintan. In: Prothero, D.R., Emry, R.J. (Eds.), The Terrestrial Eocene–Oligocene Transition in North America. Cambridge University Press, Cambridge, pp. 52–74.

Wang, H., Follmer, L.R., 1998. Proxy of monsoon seasonality in carbon isotopes from paleosols of the southern Chinese Loess Plateau. Geology 26, 987–990.

Watson, G.S., 1956. A test for randomness of directions. Monthly Notices of the Royal Astronomical Society Geophysical Supplement 7, 160–161.

Webb, T.I., Ruddiman, W.F., Street-Perrott, F.A., Markgraf, V., Kutzbach, J.E., Bartlein, P.J., Wright Jr., H.E., Prell, W.L., 1993. Climatic changes during the past 18,000 years: regional syntheses, mechanisms, and causes. In: Wright Jr., H.E., Kutzbach, J.E., Webb III, T., Ruddiman, W.F., Street-Perrott, F.A., Bartlein, P.J. (Eds.), Global Climates since the Last Glacial Maximum. University of Minnesota Press, Minneapolis, pp. 514–535.

West, R.M., 1970. Sequence of mammalian faunas of Eocene age in the northwern Green River Basin, Wyoming. Journal of Paleontology 44, 142–147.

Wilf, P., 2000. Late Paleocene–early Eocene climate changes in southwestern Wyoming: paleobotanical analysis. Geological Society of America Bulletin 112, 292–307.

Wing, S.L., Bao, H., Koch, P.L., 2000. An early Eocene cool period? Evidence for continental cooling during the warmest part of the Cenozoic. In: Huber, B.T., MacCleod, K., Wing, S.L. (Eds.), Warm Climates in Earth History. Cambridge University Press, Cambridge, pp. 197–238.

Woodburne, M.O., Swisher, C.C., 1995. Land mammal high-resolution geochronology, intercontinental overland dispersals, sea level, climate, and vicariance. In: Berggren, W.A., Kent, D.V., Aubry, M.-P., Hardenbol, J. (Eds.), Geochronology, Time Scales and Global Stratigraphic Correlation. SEPM Special Publication, 54, pp. 335–364.

Zachos, J.C., Stott, L.D., Lohmann, K.C., 1994. Evolution of early Cenozoic marine temperatures. Paleoceanography 9, 353–387.

Zijderveld, J.D.A., 1967. A.C. demagnetization of rocks: analysis of results. In: Collinson, D.W., Creer, K.M., Runcorn, S.K. (Eds.), Methods of Palaeomagnetism. Elsevier, Amsterdam, pp. 254–286.

Zonneveld, J.-P., Gunnell, G.F., Bartels, W.S., 2000. Early and middle Eocene fossil vertebrates from the western Green River Basin, Lincoln and Uinta Counties, Wyoming. Journal of Vertebrate Paleontology 20, 369–386.